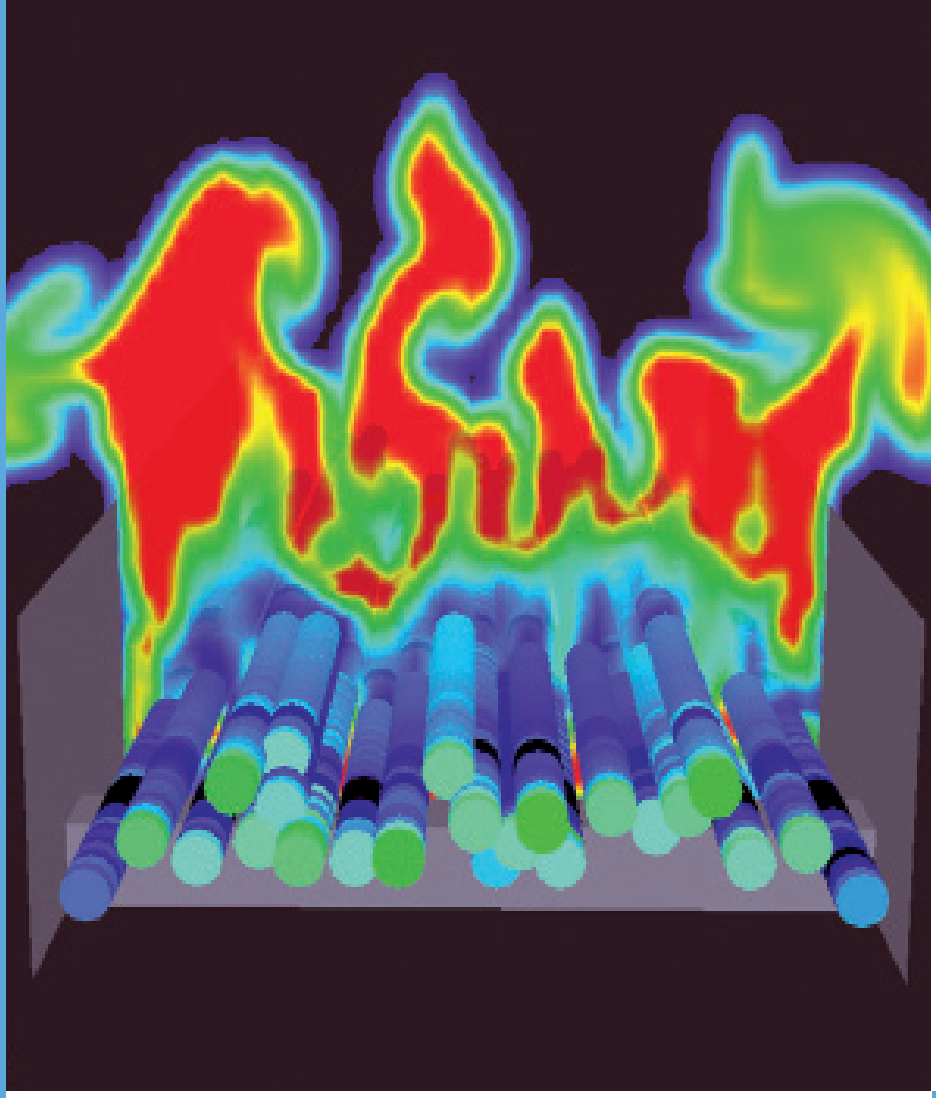

SCIENCE • TECHNOLOGY • RESEARCH HIGHLIGHTS • VISIONS •

Dissertation
44

Methods and applications of pyrolysis modelling for polymeric materials

Anna Matala

VTT

VTT SCIENCE 44

Methods and applications of pyrolysis modelling for polymeric materials

Anna Matala

Thesis for the degree of Doctor of Science (Technology) to be presented with due permission for public examination and criticism in Otakaari 1, at Aalto University School of Science, on the 15.11.2013 at 12 noon.

ISBN 978-951-38-8101-6 (Soft back ed.)
ISBN 978-951-38-8102-3 (URL: http://www.vtt.fi/publications/index.jsp)

VTT Science 44

ISSN-L 2242-119X
ISSN 2242-119X (Print)
ISSN 2242-1203 (Online)

JULKAISIJA – UTGIVARE – PUBLISHER

VTT
PL 1000 (Tekniikantie 4 A, Espoo)
02044 VTT
Puh. 020 722 111, faksi 020 722 7001

VTT
PB 1000 (Teknikvägen 4 A, Esbo)
FI-02044 VTT
Tfn. +358 20 722 111, telefax +358 20 722 7001

VTT Technical Research Centre of Finland
P.O. Box 1000 (Tekniikantie 4 A, Espoo)
FI-02044 VTT, Finland
Tel. +358 20 722 111, fax +358 20 722 7001

Kopijyvä Oy, Kuopio 2013

Methods and applications of pyrolysis modelling for polymeric materials

Pyrolyysimallinnuksen metodeita ja sovelluksia polymeereille. **Anna Matala.** Espoo 2013. VTT Science 44. 85 p. + app. 87 p.

Abstract

Fire is a real threat for people and property. However, if the risks can be identified before the accident, the consequences can be remarkably limited. The requirement of fire safety is particularly important in places with large number of people and limited evacuation possibilities (e.g., ships and airplanes) and for places where the consequences of fire may spread wide outside of the fire location (e.g., nuclear power plants).

The prerequisite for reliable fire safety assessment is to be able to predict the fire spread instead of prescribing it. For predicting the fire spread accurately, the pyrolysis reaction of the solid phase must be modelled. The pyrolysis is often modelled using the Arrhenius equation with three unknown parameters per each reaction. These parameters are not material, but model specific, and therefore they need to be estimated from the experimental small-scale data for each sample and model individually.

The typical fuel materials in applications of fire safety engineers are not always well-defined or characterised. For instance, in electrical cables, the polymer blend may include large quantities of additives that change the fire performance of the polymer completely. Knowing the exact chemical compound is not necessary for an accurate model, but the thermal degradation and the release of combustible gases should be identified correctly.

The literature study of this dissertation summarises the most important background information about pyrolysis modelling and the thermal degradation of the polymers needed for understanding the methods and results of this dissertation. The articles cover developing methods for pyrolysis modelling and testing them for various materials. The sensitivity of the model for the modelling choices is also addressed by testing several typical modeller choices. The heat release of unknown polymer blend is studied using Microscale Combustion Calorimetry (MCC), and two methods are developed for effectively using the MCC results in building an accurate reaction path. The process of pyrolysis modelling is presented and discussed. Lastly, the methods of cable modelling are applied to a large scale simulation of a cable tunnel of a Finnish nuclear power plant.

The results show that the developed methods are practical, produce accurate fits for the experimental results, and can be used with different materials. Using these methods, the modeller is able to build an accurate reaction path even if the material is partly uncharacterised. The methods have already been applied to simulating real scale fire scenarios, and the validation work is continuing.

Keywords pyrolysis modelling, simulation, polymer, cables, composites, probabilistic risk assessment (PRA)

Pyrolyysimallinnuksen metodeita ja sovelluksia polymeereille

Methods and applications of pyrolysis modelling for polymeric materials. **Anna Matala.** Espoo 2013. VTT Science 44. 85 s. + liitt. 87 s.

Tiivistelmä

Tulipalot aiheuttavat todellisen uhan ihmisille ja omaisuudelle. Mikäli riskit voidaan tunnistaa jo ennen onnettomuutta, tulipalon ikäviä seurauksia voidaan rajoittaa. Paloturvallisuuden merkitys korostuu erityisesti paikoissa, joissa on paljon ihmisiä ja rajoitetut evakuointimahdollisuudet (esim. laivat ja lentokoneet), ja laitoksissa, joissa tulipalon seuraukset voivat levitä laajalle palopaikan ulkopuolellekin (esim. ydinvoimalaitokset).

Jotta materiaalien palokäyttäytymistä voitaisiin luotettavasti tarkastella erilaisissa olosuhteissa, pitää palon leviäminen pystyä ennustamaan sen sijaan, että paloteho määrättäisiin ennalta. Palon leviämisen ennustamiseksi täytyy materiaalin kiinteän faasin pyrolyysireaktiot tuntea ja mallintaa. Pyrolyysi mallinnetaan usein käyttäen Arrheniuksen yhtälöä, jossa on kolme tuntematonta parametria jokaista reaktiota kohti. Nämä parametrit eivät ole materiaali- vaan mallikohtaisia, ja siksi ne täytyy estimoida kokeellisista pienen mittakaavan kokeista jokaiselle näytteelle ja mallille erikseen.

Paloturvallisuusinsinöörin kannalta erityisen hankalaa on, että palavat materiaalit eivät useinkaan ole hyvin määriteltyjä tai tunnettuja. Esimerkiksi sähkökaapeleiden polymeeriseokset voivat sisältää suuria määriä erilaisia lisäaineita, jotka vaikuttavat materiaalin palokäyttäytymiseen merkittävästi. Kemiallisen koostumuksen tunteminen ei ole välttämätöntä luotettavan mallin aikaansaamiseksi, mutta aineen lämpöhajoaminen ja erityisesti palavien kaasujen vapautuminen tulisi tuntea tarkasti.

Väitöskirjan tiivistelmäosa kokoaa yhteen tärkeimmät taustatiedot pyrolyysimallinnuksen ja polymeerien palokäyttäytymisen ymmärtämisen tueksi. Tässä väitöstyössä on kehitetty menetelmiä pyrolyysiparametrien estimoimiseksi ja näitä metodeita on testattu erilaisilla materiaaleilla. Mallinnusvalintojen merkitystä mallin tarkkuuteen on myös tutkittu herkkyysanalyysin keinoin. Osittain tuntemattomien polymeeriseosten lämmön vapautumista on tutkittu käyttäen mikrokalorimetria. Mikrokalorimetritulosten hyödyntämiseksi kehitettiin kaksi metodia, joiden avulla voidaan saada aikaan entistä tarkempia reaktiopolkuja. Lopuksi pyrolyysimallinnusta on hyödynnetty sovellusesimerkissä suomalaisen ydinvoimalan kaapelitilan täyden mittakaavan kaapelisimuloinneissa.

Tulokset osoittavat, että tässä työssä kehitetyt menetelmät ovat käytännöllisiä, tuottavat riittävän tarkkoja sovituksia koetuloksille ja niitä voidaan soveltaa monien erilaisten materiaalien mallintamiseen. Näitä menetelmiä käyttämällä mallintaja pystyy mallintamaan tuntemattomienkin materiaalien palokäyttäytymistä riittävän tarkasti. Menetelmiä on jo sovellettu todellisten, suuren mittakaavan palotilanteiden simuloimiseksi, ja validointityö jatkuu edelleen.

Avainsanat pyrolyysimallinnus, simulaatiot, polymeerit, kaapelit, komposiitit, todennäköisyyspohjainen riskianalyysi (PRA)

Preface

In spring 2007 I returned home from a job interview full of excitement; I had been offered a summer job at the fire research team of VTT. I did not know much about the work itself, but what could be "hotter" than a summer job playing with fire and even getting paid for it! That summer I implemented the first version of my genetic algorithm application for Matlab that has been extensively used throughout this dissertation work. After the summer job, I progressed to be a Master's thesis worker in the same team, and after graduation the work continued naturally towards the PhD dissertation (I don't think anyone even asked me if I was interested in doing a PhD, it just happened). During these years, I have had the opportunity to get familiar with the fascinating topic of fire and pyrolysis modelling, and had an opportunity to get to know many inspiring people. The learning has not been fully successful – I still burn my fingers regularly, both at work and at home, but I still love watching fire and burning things; who wouldn't?

There are so many great people I want to thank for contributing to my dissertation. First of all, I would like to acknowledge my Professor Harri Ehtamo from Aalto University School of Science, for supervising this PhD work, and the pre-examiners, Dr. Richard E. Lyon and Dr. Brian Lattimer, for their valuable comments. I would like to thank my thesis advisor and boss, Dr. Simo Hostikka from VTT, who has been supervising my work at VTT ever since the summer of 2007. He has provided continuous support, patiently provided answers to my never-ending questions and motivated me when my own ideas wained. At VTT, I'm also grateful to our technology manager Dr. Eila Lehmus, for making this doctoral work possible and for her encouragement, Dr. Esko Mikkola for his valuable comments on my dissertation manuscript and for being the best office mate, and Dr. Johan Mangs and Dr. Tuula Hakkarainen for guidance and company during the long hours of experimental work. My team (past and current) deserves a special acknowledgement for the great work ambience, and for making it easy and pleasant place to work; thank you Simo, Tuula, Esko, Johan, Topi, Antti, Terhi, Timo, Jukka, Kati, Tuomo, Peter and Tuomas. From VTT expert services, I would like to thank Mr. Konsta Taimisalo for sharing some of his endless knowledge on the experimental work and his help during the tests, and also Ms. Hanna Hykkyrä and Ms. Katja Ruotanen for their help with experimental work as well as the out of hours activities.

I had the opportunity to spend a year in the University of California, Berkeley, Department of Mechanical Engineering. I am grateful to Professor Carlos Fernandez-Pello for his supervision during that time, introducing me to many important people and for making sure I did not return home without getting tanned. I would also like to thank Dr. Chris Lautenberger for the cooperation, discussions and, most importantly, the trips to the Wine County and Lake Tahoe. Thanks to Nikki, for making Guifré and me feel so welcome. Thanks to David and Erin Rich for welcoming us to their house during the first week, for lending a bed and for the good times in their beautiful garden. I would like to thank Sonia and Laurence for being my 'Berkeley sisters', I miss you a lot. Thanks to everyone in and outside the lab (Diana!), you all made my stay in California very special!

I would like to thank Dr. Kevin McGrattan from NIST for the discussions, support and help related to FDS. I also greatly appreciate the experimental data I received from the CHRISTIFIRE project. I also acknowledge Dr. Tuula Leskelä from Aalto University School of Chemical Technology for performing the STA experiments for several materials. I would like to thank Dr. Sophie Cozien-Cazuc from Cytec, Dr. Per Blomqvist from SP, and Mr. Iván Sánchez from Gaiker, for providing samples, experimental results and support on the composites.

I'm grateful to my entire family for support, opportunities, and, most importantly, absolute love at all the phases of this work and of my life. Thank you Mum and Neville, Dad and Aulikki, Roser and Angel, Saara, Raakku, Guillem and Rommi, as well as my grandparents, cousins and other relatives. Thanks to all my friends for always being there for me, for the dinners and brunches, evenings with dance or guitar hero, walks and skiing, and all the other things I have had a pleasure to share with you. I couldn't have done this without you. Lastly, thanks to my awesome husband, Guifré, for his love and support. He believed in me when I lost the motivation, helped with all the details of this dissertation, and took me out to run when I started to climb the walls. You are the best thing that ever happened to me. T'estimo.

The work on this thesis has been mainly done in three major projects: SAFIR2010, SAFIR2014 and FIRE-RESIST. The two first are partially funded by The State Nuclear Waste Management Fund (VYR) and the third is part of the Seventh Framework Programme of European Commission. I'm also grateful to the strategic research funding of VTT for supporting the research and writing of this dissertation.

Espoo, October 10, 2013
Anna Matala

Academic dissertation

Supervisor	Professor Harri Ehtamo Aalto University School of Science Systems Analysis Laboratory Finland
Instructor	Doctor Simo Hostikka VTT Technical Research Centre of Finland
Reviewers	Doctor Richard E. Lyon, Federal Aviation Administration, USA Associate Professor Brian Y. Lattimer, Virginia Tech, USA
Opponent	Professor Richard Hull, University of Central Lancashire, UK

List of publications

This thesis is based on the following original publications which are referred to in the text as I–V. The publications are reproduced with kind permission from the publishers.

I. Matala, A., Hostikka, S. and Mangs, J. (2008) Estimation of Pyrolysis Model Parameters for Solid Materials Using Thermogravimetric Data. Fire Safety Science – Proceedings of the Ninth International Symposium, International Association for Fire Safety Science, pp. 1213–1224.

II. Matala, A., Lautenberger, C. and Hostikka, S. (2012) Generalized direct method for pyrolysis kinetic parameter estimation and comparison to existing methods. Journal of Fire Sciences, Vol. 30, No. 4, pp. 339–356.

III. Matala, A. and Hostikka, S. (2011) Pyrolysis Modelling of PVC Cable Materials. Fire Safety Science – Proceedings of the Tenth International Symposium, International Association for Fire Safety Science, pp. 917–930.

IV. Matala, A. and Hostikka, S. (2013) Modelling polymeric material using Microscale combustion calorimetry and other small scale data. Manuscript submitted to Fire and Materials in June 2013.

V. Matala, A. and Hostikka, S. (2011) Probabilistic simulation of cable performance and water based protection in cable tunnel fires. Nuclear Engineering and Design, Vol. 241, No. 12, pp. 5263–5274.

Author's contributions

Matala is the main author of all the publications I–V and has performed most of the work reported in the articles.

In Publication I, the author developed a Matlab tool for data processing and genetic algorithm application. She also performed the parameter estimations using the tool for several materials reported in the article.

In Publication II, the author developed an analytical method for estimating the kinetic parameters of pyrolysis reaction together with Lautenberger. Lautenberger was responsible for the parameter estimations using estimation algorithms while the author estimated the parameters using analytical methods.

In Publication III, the author estimated all the parameters, performed the sensitivity study of the modelling choices, and participated in performing the cone calorimeter experiments.

In Publication IV, the author developed the method for using the Microscale Combustion Calorimetry and tested it using generated and experimental data.

In Publication V, the author did the material parameter estimation for the cable, estimated the sprinkler parameters using experimental results and performed the Monte Carlo simulations using different water suppression configurations. She also participated to the cone calorimeter experiments of the cable, and designed and performed the water distribution tests for nozzles together with Hostikka.

Contents

List of Figures

List of Tables

List of Symbols

A	Pre-exponential factor
c_p	Specific heat
E	Activation energy
f	Reaction model
ΔH	Heat of reaction
ΔH_c	Heat of combustion
k	Thermal conductivity
k_r	Reaction constant
m	Mass
$\dot{m}$	Mass loss rate
M	Experimental result
N	Reaction order
N_k	Number of experimental results
N_{O_2}	Reaction order of oxygen concentration
Q	Total heat release
$\dot{q}$	Heat release rate
R	Universal gas constant
T	Temperature
t	Time
x	Depth
Y	Mass fraction / Oxygen concentration
y	yield
Z	Residue yield

Greek

α	Fractional conversion of mass
β	Heating rate
δ	Thickness / Scaling factor
ϵ	Emissivity
κ	Absorption coefficient
μ	Mean of the heating rates
ρ	Density

Subscripts

0	Initial value
exp	Experimental
F	Fuel gas
I	Inert gas
i	Component index / Time step
j	Reaction index
k	Exp. result index (in GA)
mod	Model
Z	Residue

List of Abbreviations

ATH	Alumina trihydrate
CaCl	Calcium Chloride
$CaCO_3$	Calcium Carbonate
CFD	Computational Fluid Dynamics
DM	Direct method
DOP	Diethylhexyl Phthalate
DPO	Diphenyl oxide
DSC	Differential Scanning Calorimetry
FDS	Fire Dynamics Simulator
FEM	Finite Element Method
GA	Genetic Algorithm
GDM	Generalized Direct Method
HCl	Hydrochloric acid
HGA	Hybrid Generic Algorithm
HRR	Heat release rate
LH	Latin Hypercubes
MC	Monte Carlo
MCC	Microscale Combustion Calorimeter
MD	Molecular dynamics
MDH	Magnesium hydroxide
MLR	Mass loss rate
NPP	Nuclear power plant
PFS	Probabilistic Fire Simulator
PMMA	Poly(methyl methacrylate)
PRA	Probabilistic Risk Assessment
PVC	Polyvinyl Chloride
SA	Simulated Annealing
SCE	Suffled Complex Evolution
SGS	Sub-grid-scale
SHC	Stochastic Hill Climber
TGA	Thermogravimetric Analysis

1. Introduction

1.1 Background

Fire causes significant harm to people and property. In Finland, on average 100 people (about 18 per million citizens) die every year through fire, although the trend has been descending in recent years. Deaths due to fires initiated from smoking or careless handling of fire decreased in 2007–2010, but the number of fires caused by vandalism rose [1]. Although most fires that lead to death occur in residential buildings, the potential consequences of fire become especially serious in public places with high occupation yet limited evacuation possibilities, such as on aeroplanes [2] or ships [3]. Fires in industry may arise for various reasons, including failing electronic components, dust, or vandalism, and cause significant expenses to the owners and insurance companies.

In general, the objective of fire safety engineering is to protect first people and animals, then property and the fire fighters. In some safety critical facilities, such as nuclear power plants (NPP), these objectives are not enough: one must also consider the environmental problems caused by leaking radioactive material or the economic losses of industry that are caused by the attendant lack of power. Fire at a nuclear power plant is considered to be among *initiating events* (events that could begin a chain of events leading to a serious accident) in *probabilistic risk assessment* (PRA); therefore it is a focus of extensive research [4].

In the earlier times, building materials were limited to those available more directly from nature: wood, stone, and metals. Entire cities of wooden houses easily burnt to the ground, and iron structures rust away and fall down. In the 20th century, however, new materials started to emerge. The use of polymers and synthetic fibres increased in the manufacturing of furnitures and other household goods. As electronics grew more and more commonplace, kitchens and living rooms became filled with new gadgets and cables of various types. Cables also account for a significant proportion of the fire load at factories and power plants.

The search for better materials led to the development of modern composites. In transportation, the composites were designed to be lighter, less expensive, stiffer, or stronger than the original metal. These qualities make composites very attractive, especially in, for example, the aviation industry. More than 50% of the structure of an Airbus 380 is made of composite materials [5]. Unfortunately, the fire performance of these new materials does not always improve

on (or even equal) that of the traditional materials. A laminate loses its structure when heated, and in a polymer composite only parts of the material survive the fire. A glass fibre reinforced phenolic composite after a fire is shown in Figure 1.1. The structure is weakened by the pyrolysis of the phenolic polymer and the subsequent delamination.

Clearly, the new materials needed protection from the heat. That is why several flame retardant additives have been developed over the years. Some materials are flame retardant by nature, such as charring wood or materials that release non-combustible gas that cools the surface and dilutes the combustion gases (as halogen in polyvinyl chloride (PVC) does). Halogenated flame retardants are not recommended nowadays, because of environmental concerns, but a similar mechanism has been adopted for new, non-corrosive flame retardants that release, for example, water [6, 7]. Wood charring has also inspired new, intumescent surfaces that protect the underlying surface from the heat [8].

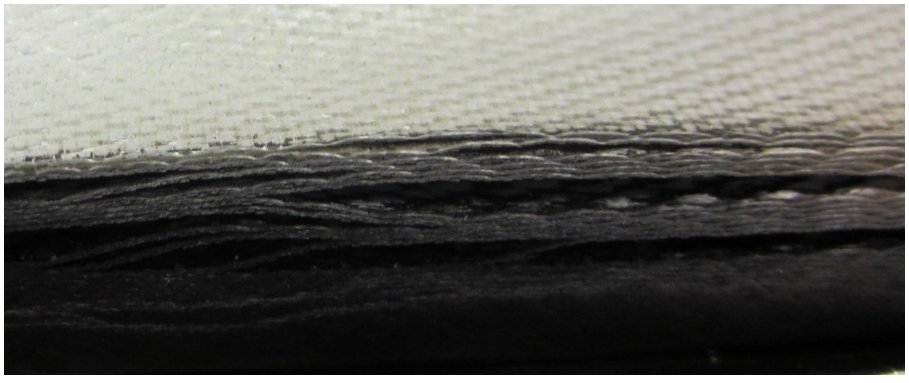

Figure 1.1. Glass fibre-Phenolic composite after fire.

Fire simulations are used extensively in the planning and design of new solutions for structures or interiors of buildings. They can be used as an element of performance-based design, wherein the designer has to prove that the new solution is at least as safe as the previously accepted solutions. They can also be used as part of the PRA of nuclear power plants [4].

Increased processing capacity and improvements to software have made extensive fire simulations possible. The simulations can be used to predict fire spread and/or its consequences and to study structural performance [9], the water suppression [10], evacuation safety [11], or even the human behaviour [12]. Studies of the thermal degradation at atomic level have been done by means of molecular dynamics (MD) [13].

Pyrolysis modelling is an important part of a modern fire simulation. Traditionally, the consequences of fire have been evaluated on basis of pre-described

fires and standard fire curves. Pyrolysis modelling is designed to predict the heat release rate and the response of the structures and materials that follows. It allows implementation of more realistic fire scenarios and study of the flame spread.

In the future, pyrolysis modelling may also be used in product development for new materials. Potential fire risks and the structures' performance in fire could be evaluated by means of simulations before manufacture of large samples. Pyrolysis modelling can also be part of the process of optimisation of the new materials' properties. This could be especially useful in development of new flame retardant materials or mechanisms.

Pyrolysis modelling consists of five steps:

1. The material is tested experimentally on small scale. Typical experimental methods in this connection are thermogravimetric analysis (TGA) [14,15] and cone calorimeter [16].
2. The experiments are described by a mathematical model. The pyrolysis is often modelled by means of Arrhenius equation in combination with data on heat transfer [17,18]. The model's validation is an important part of the process.
3. The model has to be solved numerically and this solution verified.
4. Model parameters are often unknown and have to be estimated by fitting of the model to the experimental results.
5. The pyrolysis model is taken in combination with the computational fluid dynamics (CFD) calculations. This is the case with the Fire Dynamics Simulator (FDS) [18].

The present work concentrates on finding methods for estimation of the pyrolysis parameters, an important topic since the model parameters are not always well-known or even well-defined sets for any given material. They may vary significantly, depending on the model's limitations and complexity. Therefore, they cannot be listed in any handbook or on a product sheet. The most significant difference between the work of a fire safety engineer and a product R&D engineer is that the fire safety engineer does not usually have precise information about the fuel or fire load. There is a demand for methods that are accurate enough for predicting the material degradation correctly and at the same time are simple and fast enough that they can be easily used by a practising fire engineer.

Several methods have been developed for extracting the reaction (or *kinetic*) parameters from the experimental data, some simple and fast and others more complicated but providing more accurate results. The other (*thermal*) parameters are typically estimated from bench scale data [19] or in some cases measured directly [20]. Publication I and Publication II cover the authors contri-

bution to the estimation methods and Publication III describes the sensitivity study for the modelling choices.

This dissertation provides methods for pyrolysis modelling of these complex materials. It also offers methods for calculating the reaction specific heat release rate that can in some cases be used in estimation of the material composition (in Publication IV).

Not only the material parameters, but also the geometry and structure, additives and flame retardants may cause challenges in larger scale simulations with complex materials such as cables or composites. The methods are applied to a real fire safety assessment for a nuclear power plant in Publication V.

The work on this dissertation was carried out primarily in two projects. The material modelling of the cables for improving nuclear power plant fire safety has been developed as part of the Finnish Research Programme on Nuclear Power Plant Safety (SAFIR 2010[1] and SAFIR 2014[2]) [4]. The work pertaining to composites is done as part of the European Union project FIRE-RESIST[3].

1.2 Outline of the dissertation

The dissertation is organised as follows:

Chapter 2 provides the background on the work done for this dissertation. First, the pyrolysis model and other important equations for the material modelling are reviewed. Then the experimental methods used for the parameter estimation are presented. Literature on some significant estimation methods is reviewed. Also, the Monte Carlo method is presented in brief.

Chapter 3 presents some special cases of pyrolysis modelling, including thermoplastic and thermoset polymers and intumescent surfaces. It also provides a literature review considering some complex materials (PVC, cables, and composites) and the associated modelling.

Chapter 4 summarises the methods developed by the author in the course of the doctoral research. First, the FDS models of the experimental methods are briefly described. After this, the applications of the two estimation methods (one analytical and one a curve fitting algorithm) are discussed, after which an application of new experimental method that can be used in parameter estimation, *microscale combustion calorimetry* (MCC), is presented.

Chapter 5 summarises the most important results emerging in Publications I–V and some additional discussion related to the topics of this work.

Chapter 6 presents conclusions and discussion of the topic of the dissertation. Future plans and possibilities for applications are presented.

[1] See http://virtual.vtt.fi/virtual/safir2010/
[2] See http://virtual.vtt.fi/virtual/safir2014/
[3] See http://www.fire-resist.eu/FireResist/index.xhtml

2. Pyrolysis modelling and fire simulations

2.1 Motivation

If one is to be able to predict the spread of fire, the pyrolysis model, starting with the solid phase degradation reactions, has to be defined. This chapter provides background information and the literature survey needed for understanding of the concepts of pyrolysis modelling. First, a brief review of the pyrolysis model and the equations needed for predicting the fire spread of a material are presented. Then the experimental methods essential to the pyrolysis modelling are described. An review of literature on existing parameter estimation methods is provided and discussed in brief. The methods applied and improved upon for Publication I and Publication II are based on these methods. Lastly, the Monte Carlo simulation method is presented as it is relevant for an understanding of Publication V.

2.2 The pyrolysis model

Pyrolysis is the thermal degradation that occurs in the solid phase of a material when it is heated. The bonds between the molecules start to break at elevated temperatures, leading to release of volatile compounds and changes from the original structure of the material. This is seen as mass loss. Technically, 'pyrolysis' refers only to thermal degradation without oxygen; in general (regardless of the oxygen concentration) the mechanism is called thermolysis. In the presence of air, the carbonous residue may oxidise. The combustible gases released during the pyrolysis may also ignite, leading to combustion in the gas phase. This increases the gas temperature, with the results being slightly faster degradation than in inert ambient. In this dissertation, the term 'pyrolysis' is used to describe the thermal degradation at elevated temperatures both in inert ambient and in the presence of oxygen.

The temperature dependent reaction rate of the pyrolysis is often described by the Arrhenius equation. This equation describes the temperature dependence of reaction constant

$$k_r = Ae^{-\frac{E}{RT}}, \tag{2.1}$$

where A is the pre-exponential factor, E the activation energy, R the universal gas constant, and T temperature. Originally developed by Svante Arrhenius

in 1884 in study of the dissociation of electrolytes [21], the equation has been applied since then in various fields of research, from chemical and physical processes to studies of quantum statistics and climate change [21–28]

In the fire community interest in the Arrhenius parameters grew in the late 20th century, first for describing the char oxidation [29–31] and then for predicting the thermal decomposition in the solid phase [17–19].

The equation gives a relationship between reaction rate and temperature and is often represented in the form

$$r_j = \frac{d\alpha}{dt} = A_j f(\alpha) e^{-\frac{E_j}{RT}}, \tag{2.2}$$

where $\alpha = (m_0 - m)/(m_0)$ is the fractional conversion from reactants to products ranging from 0 to 1, and T the temperature of the solid. The so called *kinetic triplet* consists of A_j, E_j, and reaction model $f(\alpha)$. Each reaction j has a different kinetic triplet. The reaction model often depends on reaction order N_k and may be expressed as

$$f(\alpha) = (1 - \alpha)^{N_j}. \tag{2.3}$$

The stoichiometric reaction orders of chemical reactions are integers (usually 1). The thermal degradation is a consequence of the chemical bonds breaking at elevated temperatures. The materials consist of several, different bonds, requiring different amounts of energy for breaking. The overall mass loss reaction is, therefore, a combination of several chemical reactions. In pyrolysis modelling, these reactions are lumped together and hence fractional reaction rates also are used. The model is not an attempt to describe each chemical reaction exactly; the parameters should be considered model specific elements that merge the net effect of several overlapping reactions.

The reaction rate depends on the temperature. The temperature at the front surface of the material rises through by radiation and convection, while inside the material the heat is transferred via conduction and internal radiation. A one dimensional heat conduction equation with internal heat generation/absorption is often sufficient to determine the temperature gradient, $T(x)$:

$$\rho c_p \frac{dT}{dt} = \frac{\partial}{\partial x} k \frac{\partial T}{\partial x} + \dot{q}_s^{'''}, \tag{2.4}$$

where ρ is the solid density, c_p the specific heat capacity, k thermal conductivity, x depth from the surface and $\dot{q}_s^{'''}$ a source term that consists of the chemical reactions ($\dot{q}_{s,c}^{'''}$) and the radiation and emission at depth ($\dot{q}_{s,r}^{'''}$). The chemical

source term is linked to the Arrhenius equation by the reaction rate:

$$\dot{q}_{s,c}^{'''} = -\rho_0 \sum_j r_j(x) \Delta H_j, \tag{2.5}$$

where ΔH_j is the heat of reaction of reaction j.

The boundary condition at front (F) surface is

$$-k \frac{\partial T}{\partial x}(0,t) = \dot{q}_c^{''} + \dot{q}_r^{''}, \tag{2.6}$$

where convective heat flux $\dot{q}_c^{''}$ is

$$\dot{q}_c^{''} = h(T_g - T_F); \tag{2.7}$$

constant h is the heat transfer coefficient, and the net radiative flux is

$$\dot{q}_r^{''} = \dot{q}_{r,in}^{''} - \epsilon \, \sigma \, T_F^4, \tag{2.8}$$

where ϵ is the emissivity and σ the Stefan-Boltzmann coefficient. [14, 18]

In the presence of air, the combustible gases released during pyrolysis may ignite and lead to combustion. This is modelled through assumption of a component specific heat of combustion (ΔH_c) that describes the heat released per unit mass. The heat release rate per unit area then becomes

$$\dot{q}^{''} = \dot{m}^{''} \Delta H_c = \Delta H_c \int_0^L \sum_j \sum_i A_{i,j} \rho_i e^{-E_{i,j}/RT(x)} dx, \tag{2.9}$$

where i is the component (material) index and j reaction index.

Materials that can sustain smouldering combustion are porous and form solid carbonaceous char when heated. Materials that melt do not exhibit this kind of combustion. The char is formed on the exposed surface. When the char is oxidised in this region, a glow at high temperatures (about $600°$C for wood) results. This exothermic process yields ash and residual char, along with volatile products (e.g., tar) that have high carbon monoxide content. These products are also flammable if accumulating in a closed space; hence, smouldering may lead to flaming after passage of considerable time. [14]

Surface oxidation is most significant after the flame is extinguished, but the surface is still hot, for example, after combustion of lignocellulosic material. An example of the surface oxidation is seen in Figure 2.1. A graphite sample was tested in TGA and differential scanning calorimetry (DSC) under both oxidative (air) and inert (nitrogen) ambient conditions (see Section 2.3 for more details). In the presence of oxygen, the sample degrades almost completely (leaving less than 1% as residue). Without oxygen, this degradation does not occur, even at

high temperatures and with a slow heating rate. Similarly, the DSC experiments show a clear exothermic reaction peak for the sample in air, while the same test in nitrogen does not show any reaction (except minor experimental fluctuation of the baseline).

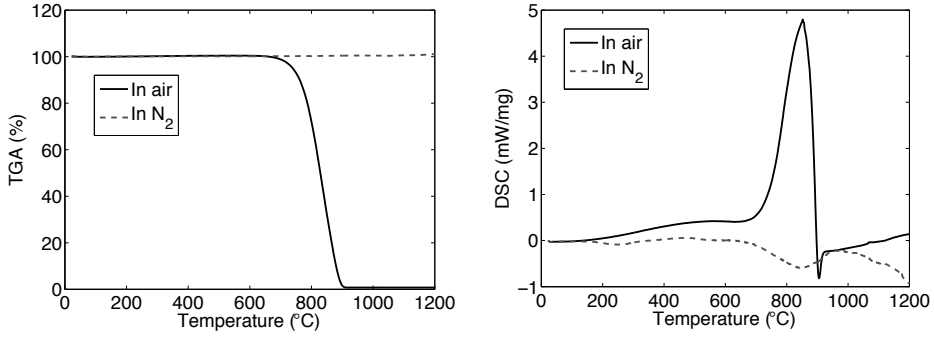

Figure 2.1. a) TGA and b) DSC experiments with graphite in air and in nitrogen at $2\,\mathrm{K/min}$.

A reaction depending on the oxygen concentration can be modelled by means of a modified Arrhenius equation:

$$r_{O_2,j} = A_j(1-\alpha_j)_j^N \exp\left(-\frac{E_j}{RT}\right) Y_{O_2}^{N_{O_2}}, \tag{2.10}$$

where Y_{O_2} is the oxygen concentration and N_{O_2} is the reaction order of the oxygen concentration. If reaction rate does not depend on oxygen concentration (as normal pyrolysis reaction), $N_{O_2} = 0$.

The material in the model consists of several *pseudo-components*. A pseudo-component (later also simply *component*) refers to a component in the model that represents one mass loss step in the model. It does not necessarily represent any particular chemical reaction, but it does serve as a way to model the net effect of all reactions occurring simultaneously. In total, there are at least 10 model parameters per reaction or component. Each component is described in terms of these parameters. Some components may encompass several reactions (or competing reactions), which increase the number of parameters still further. The parameters in the model are summarised in Table 2.1.
Several pieces of software have been developed in the fire community for modelling the thermal degradation of solids: FDS[1] [18], Gpyro[2] [19], Open Foam[3], and ThermaKin [32]. FDS and OpenFoam are CFD codes while Gpyro and

[1]See https://code.google.com/p/fds-smv/
[2]See http://code.google.com/p/gpyro/
[3]See http://www.openfoam.com/

Table 2.1. Summary of parameters of pyrolysis modelling. *Est* estimated from and *Mes* measured with. (*R*) reaction specific. (*C*) component specific.

Param.	Explanation (unit)	Eq.	Method of obtaining	**R**eaction/ **C**omponent
A	Pre-exponential factor (s^{-1})	2.2	*Est* TGA/MCC	*R*
c_p	Specific heat (kJ/(K·kg))	2.4	*Mes* DSC / *Est* cone calorimeter	*C*
E	Activation energy (J/mol)	2.2	*Est* TGA/MCC	*R*
ΔH	Heat of reaction (kJ/kg)	2.5	*Mes* DSC / *Est* cone calorimeter	*R*
ΔH_c	Heat of combustion (kJ/kg) / (MJ/kg)	2.9	*Mes* MCC / *Est* cone calorimeter	*R*
k	Thermal conductivity (W/(m· K))	2.4	*Mes* / *Est* cone calorimeter	*C*
N	Reaction order	2.2	*Est* TGA/MCC	*R*
N_{O_2}	Reaction order of oxidation	2.10	*Est* TGA results in air	*R*
ϵ	Emissivity	2.8	*Est* cone calorimeter	*C*
ρ	Density (kg/m^3)	2.4	*Meas* directly	*C*

ThermaKin are limited to the solid phase. Gpyro also includes an algorithm for estimation of the model's parameters.

2.3 Experimental methods

The experiments commonly employed in fire research can be divided into small (milligram), bench (gram to kilogram), and large/full (kilogram to metric ton) scale experiments on the basis of the sample size required. The small scale experiments are the easiest to model and involve less inaccuracy related to fire or experimental set up. The material models are typically built on the basis of small and bench scale experiments. Large scale fire tests are often very expensive, but important for code validation purposes.

2.3.1 Small scale experiments

In a small scale experiment, the sample mass is usually 1–30 mg. These experiments typically measure only one property at a time, such as mass, heat of reaction, specific heat, or heat release rate. The reaction parameters and sometimes even a good estimate as to the sample composition can be determined by means of small scale experimental results.

The most commonly used small scale experiment for pyrolysis modelling is the TGA. It uses a small furnace filled with either air or inert purge gas (often nitrogen). The sample is inside a small crucible that is placed over a load cell. During the experiment, the sample mass is measured. The experiment can be performed either *isothermally* (i.e., at a one constant temperature) or *non-isothermally* (with temperature increasing linearly). The non-isothermal experiment is often more suitable for the estimation of the pyrolysis parameters, since it also provides information about the reaction temperatures. The heating rates are relatively low (2–30 K/min), in order to keep the sample in thermal equilibrium with the furnace. [14,15] For pyrolysis modelling purposes, TGA experiments are often performed at several heating rates. This is necessary, because the chemical reactions may depend on heating rate, and using several rates enables the estimation of more general reaction parameters. An example of TGA results at several heating rates is seen in Figure 2.2. Often the increasing heating rate moves the reaction to higher temperatures. That means that the reaction takes place more slowly than the heating of the sample and therefore the temperature of the sample is higher when the mass loss occurs. At very high heating rates or with thermally thick samples the thermal equilibrium between the furnace and sample may be lost and the sample temperature no longer corresponds to the furnace temperature.

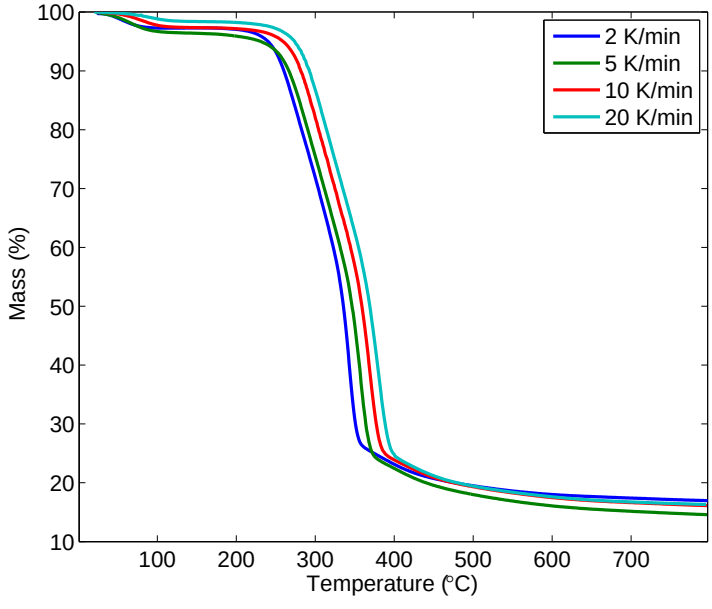

Figure 2.2. TGA results of birch wood at 2–20 K/min heating rates in nitrogen ambient.

More information about the reaction enthalpies and specific heat is provided by another small scale experiment, DSC. The furnace and the method of operation are similar those in TGA. In DSC, the sample temperature is regulated relative to a reference sample, and the required energy is measured. With DSC, one can perform experimental measurements in an individual experiment or simultaneously with TGA. From individually measured DSC, one can calculate the heat of reaction and the specific heat capacity. It is good to keep in mind that the measured value is actually the joint effect of possibly several simultaneous reactions. The results should then be scaled for the target application, more specifically, to its reaction path. [14, 15] For accurate calculation of the specific heat, three measurements are required in all: of the actual material, of a reference sample with known specific heat (often sapphire), and of an empty pan for setting of the baseline. The baseline value is subtracted from the results for the actual sample and the reference. The specific heat capacity of the reference sample is scaled by the ratio of the DSC measurements between the sample and the reference:

$$c_{p,s}(T) = \frac{\dot{q}_s/m_s(T)}{\dot{q}_r/m_r(T)} c_{p,r}(T), \tag{2.11}$$

where the subscript *r* refers to the reference and *s* to the sample.

A simpler but less accurate method is to calculate the specific heat by using only the baseline corrected heat flow of the sample. Then the heat flow for the initial mass is scaled by the current heating rate β:

$$c_{p,s} = \frac{\dot{q}_s/m_s}{\beta}. \tag{2.12}$$

A comparison of the results of these methods is shown in Figure 2.3.
The heat of reaction (or reaction enthalpy) is calculated as the integral over the reaction peak in DSC. An example of the definition of the heat of reaction is seen in Figure 2.4.

When DSC is performed simultaneously with a TGA experiment, the results are mostly more qualitative than quantitative. Often a significant, unpredictably behaving baseline can be observed in the simultaneous DSC results that make the calculation of reaction enthalpy extremely difficult. This is probably because of experimental uncertainty that comes from the set-up necessary for measuring the sample mass simultaneously with the heat flow. Qualitative results may, however, be very useful, since they reveal whether the reaction is endothermic or exothermic. In Figure 2.5, qualitative DSC results for heat flow in nitrogen and in air can be seen. Three reactions can be observed in air, two in nitrogen. The first one occurs at around $100°$C and is endothermic in both purge gas conditions. An endothermic reaction that occurs at low temperature

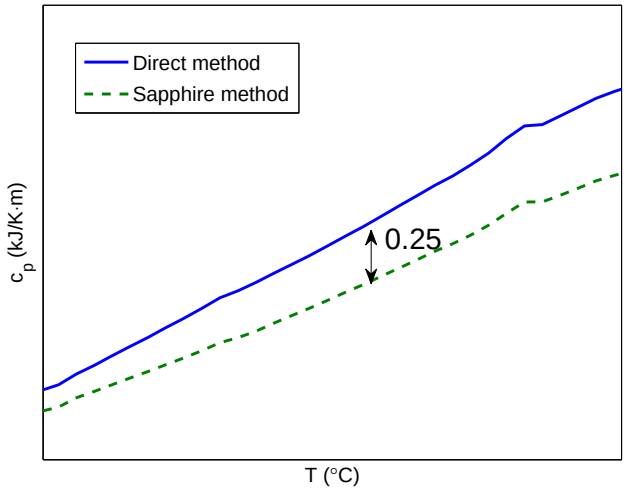

Figure 2.3. Comparison of direct method to sapphire method in calculation of specific heat from DSC results for a furane sample. Experimental data courtesy of Gaiker.

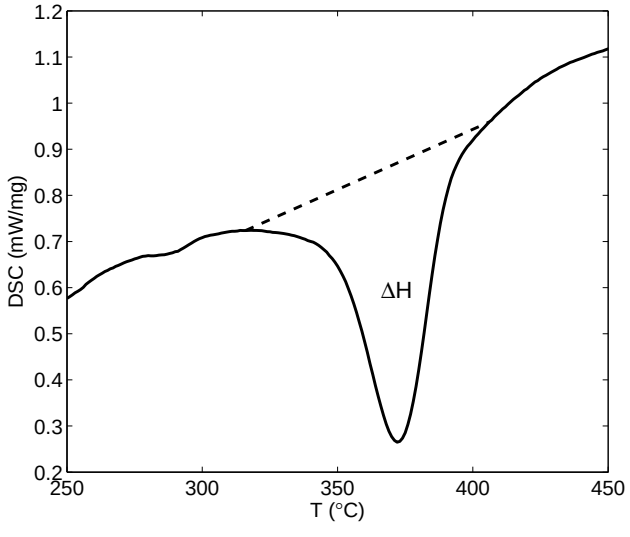

Figure 2.4. Integration over the reaction peak for determination of the heat of reaction.

can usually be identified as evaporation of moisture. The second reaction takes place after $300°$C and is exothermic in air and endothermic in nitrogen. The additional reaction only in air (peak at $440°$C) is defined as char oxidation. In the

presence of air, the exothermic peaks can indicate oxidative surface reactions or flaming combustion. It is difficult to know for certain if the combustion gases are ignited during the test or not, although self-ignition is not very probable at low temperatures. The possibility of ignition can be decreased by reducing sample size.

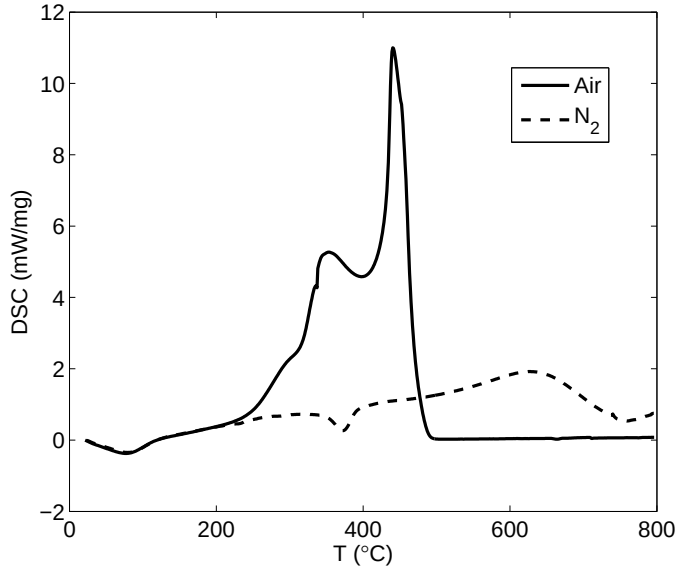

Figure 2.5. DSC results for birch at 10 K/min in air and nitrogen. Exothermic peaks are positive.

Microscale combustion calorimetry (MCC) can be used for measuring the heat release rate of a sample. It first pyrolyses the sample in a nitrogen environment, at a higher heating rate than in the TGA (typically around 60 K/min, although heating rates from 12 to 120 K/min are possible). Then the pyrolysis gases flow into a combustor, a tube whose high temperature and sufficient oxygen concentration cause all the combustible gases to burn immediately. The result is the heat of complete combustion as a function of temperature. [33, 34] The pyrolysis can alternatively be done in air, to study the oxidation of pyrolysis char. In this work, the MCC results are combined with the information from the TGA for determination of the heat of combustion values for each reaction. This information can be used when one is simulating complex materials, e.g., polymer samples. [35]

2.3.2 Bench-scale tools – the cone calorimeter

The cone calorimeter (ISO 5660-1, [16]) is the most commonly used bench-scale experimental tool in fire research. The sample usually has dimensions of 10 cm $\times$ 10 cm $\times$ 0.1–5 cm and has a substrate made of mineral-based insulation or calcium silicate board on the unexposed surface. The sample is placed under a cone shaped heater, which heats the sample with a radiant heat flux of 10–75 kW/m^2. The igniter is an electric spark that is kept on until the sample ignites, although spontaneous ignition may also be investigated without use of the spark igniter. The gases are collected in a hood, from which the various properties are measured. As a result, the cone calorimeter provides information about mass loss, heat release rate, and soot yield. Additionally, sample temperatures may be measured by means of thermocouples. The standard cone calorimeter operates in ambient air, but ambient controlled cone calorimeters are available also. They can be used for studying the effect of the oxygen in the atmosphere or the pyrolysis of the sample in an inert (nitrogen) ambient. [16, 36, 37]

2.4 Parameter estimation

The reaction rate of the thermal degradation of a material is often modelled by means of Arrhenius equation as explained in Section 2.2. The kinetic parameters cannot be measured directly; they need to be estimated somehow from the experimental data. An overview of methods to quantify kinetic parameters is provided in the following sections. The estimation algorithms presented in Subsection 2.4.2 can also be used in estimation of other (mainly thermal) model parameters.

2.4.1 Semi-analytical methods

The first methods, developed in the 1960s, included approximations, reference points, and graphical solutions [38–40]. The isoconversional (i.e. applying multiple heating rates) methods were soon discovered to be more useful because they provide more general results. They can be used for defining the reaction model ($f(\alpha)$) or the reaction parameters (A, E) [22–25]. Drawbacks to these analytical methods may be found in their limited accuracy; inconvenience of locating various reference points; limitations in reaction steps or order; or, in some cases, the fact that the complete kinetic triplet, (A, E) or $f(\alpha)$, cannot be solved from the same data set. The fire community's interest in the reaction parameters has led to some new, simple but reasonably accurate methods, aimed at encouraging modellers to base their kinetic parameters for their material

instead of using estimates from the literature [41–43].

The methods presented in this chapter assume that the pyrolysis reaction follows Eq. 2.2, or, in integral form,

$$F(\alpha) = \frac{A}{\beta} \int_{T_0}^{T} e^{-\frac{E}{RT}} dT. \tag{2.13}$$

In the 1960s, several methods were suggested for determination of the parameter pair (A,E) from experimental data [38–40]. Bell and Sizmann [38] presented an approximation for the integral,

$$\int e^{-\frac{E}{RT}} dT \approx \frac{RT^2}{E + 2RT} e^{-\frac{E}{RT}}, \tag{2.14}$$

which at two separate heating rates (β_1 and β_2 at the same conversion α, see Figure 2.6) leads to the following equation for activation energy

$$E = \frac{RT_1T_2}{T_2 - T_1} \ln\left(\frac{\beta_2}{\beta_1}\right)\left(\frac{T_1}{T_2}\right)^2. \tag{2.15}$$

They compared this approximation to an experimental method called *step annealing*. The latter is an iterative process wherein the sample is heated over time Δt_i from temperature T_i to T_{i+1} and sample concentration α_{i+1} is measured at each step i. The set (α_i, T_i) is then given by

$$\int_{\alpha_i}^{\alpha_{i+1}} \frac{d\alpha}{f(\alpha)} = e^{-\frac{E}{RT_{i+1}}} \cdot \Delta t. \tag{2.16}$$

Step annealing has since been developed into an estimation algorithm (further discussed in Subsection 2.4.2). Both methods are isoconversional, i.e., they require data at several heating rates. However, the step annealing can also be modified for just one heating rate.

Flynn and Wall [39] used an approximation technique to determine the activation energy. This method too is isoconversional. Similar to the previous method, the constant conversion is chosen for each heating rate, and the temperature is recorded (see Figure 2.6).

With the substitution $x = E/RT$, Eq. 2.13 becomes

$$F(\alpha) = \frac{AR}{\beta E} \int_{x_0}^{x_i} e^{-x} dx, \tag{2.17}$$

where $x_0 = E/RT_0$ and $x_i = E/RT_i$ and, after taking of a natural logarithm, this becomes

$$\ln(F(\alpha)) = \ln\left(\frac{AR}{E}\right) + \ln\left(\frac{1}{\beta}\right) + \ln\left(\int_{x_0}^{x_i} e^{-x} dx\right). \tag{2.18}$$

The above-mentioned authors found that for $E/RT \geq 20$, the integral can be approximated thus:

$$\ln\left(\int_{T_0}^{T_i} e^{-\frac{E}{RT}}\right) dT \approx -2.315 - 0.457\frac{E}{RT_i} \tag{2.19}$$

and therefore E becomes, after differentiation,

$$E \approx -\frac{R}{0.457}\frac{\Delta \ln(\beta)}{\Delta T^{-1}}. \tag{2.20}$$

This approximated value is then used for calculation of a more accurate estimate for E/RT and consequently its integral. This method was developed in a time when solving integrals numerically was not commonly performed. Instead, approximations and lists of integral values were used.

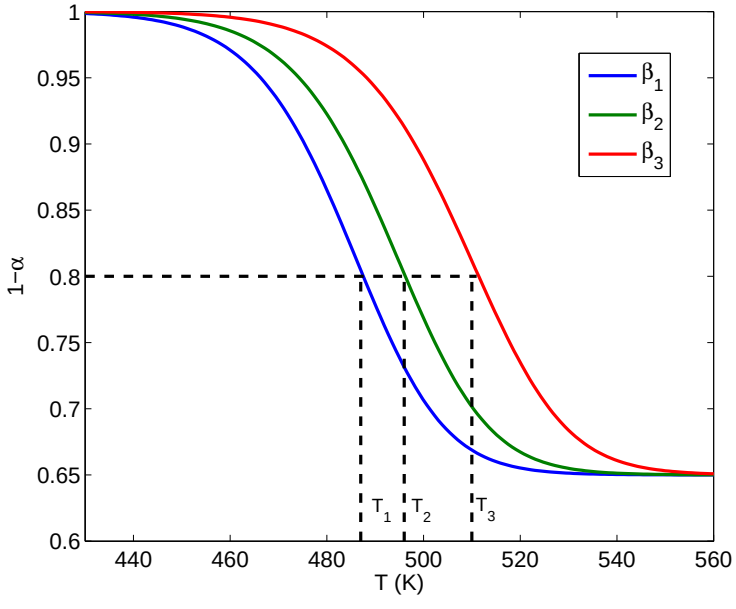

Figure 2.6. Demonstration of selecting different reference points for Flynn's isoconversional method.

Friedman [40] suggested several methods that are based on reference points and allow the use of reaction orders that are not equal to one. His methods are based on either reference points from two heating rates, or multiple points from the same data. In the simplest form, the reference point is chosen from

the point of the highest reaction rate ($\frac{d^2\alpha}{dT^2} = 0$):

$$E = NRT_p^2 \frac{(\frac{d\alpha}{dT})_p}{1-\alpha_p}. \tag{2.21}$$

Another relation, a slightly more elaborate one, requires two reference points for the same heating rate

$$E = -R \frac{\ln\left(\frac{(\frac{d\alpha}{dT})_2}{(\frac{d\alpha}{dT})_1}\right) + N\ln\left(\frac{1-\alpha_1}{1-\alpha_2}\right)}{T_2^{-1} - T_1^{-1}}. \tag{2.22}$$

Friedman also provided several relations for reaction order N that shall be discussed later in this section.

Since the 1980s, an isoconversional method that is based on linear fitting has been widely used in many fields of research in slightly different forms [22–25]. Methods in this family are also called the *model-free methods*, because they do not require an analytical form of the reaction model ($f(\alpha)$). The approach can be applied either for isothermal thermogravimetric data at several temperatures or to non-isothermal data at one heating rate.

The idea of the isothermal version is to take the natural logarithm of both sides of the Arrhenius equation. After rearrangement of the terms, it becomes

$$\ln\left(\frac{(\frac{d\alpha}{dT})}{f(\alpha)}\right) = \ln(A) - \frac{E}{RT}. \tag{2.23}$$

The left-hand side of the equation consists of the experimental values that should form a line when plotted against T^{-1} with $\ln(A)$ being the intercept and -E/R the slope. If $f(\alpha)$ depends on N, the best fit can be found through repeating of the calculation at several reaction orders, and the best fitting solution will be chosen. [22, 23]

In non-isothermal conditions, the above-mentioned method becomes a bit more complicated. If the measurement is done at only one heating rate, the results are often ambiguous. Keuleer et al. [23] suggest using the equation

$$\ln\left(\frac{\beta\,(\frac{d\alpha}{dT})}{f(\alpha)}\right) = \ln(A) - \frac{E}{RT} \tag{2.24}$$

at several heating rates (β) at fixed values of conversion α. Liu et al. [25] base their method on an approximation of the temperature integral yielding the linear relationship

$$\ln\left(\frac{\beta}{T^2}\right) = \ln\left(\frac{AR}{Eg(\alpha)}\right) - \frac{E}{RT}, \tag{2.25}$$

where $g(\alpha) = \int_0^\alpha \frac{d\alpha}{f(\alpha)} = \frac{AE}{\beta R} p(\frac{E}{RT})$.

Other related methods have been suggested and presented by several authors over the past few years [21, 24, 44–47].

The key parameter of $f(\alpha)$ for the reaction order model is the reaction order N. From the chemistry point of view for thermal degradation reactions reaction orders other than 1 do not have real meaning, as is discussed in Section 2.2. Many simplified reaction models are limited to the first order. However, the reaction order does affect the reaction rate shape significantly, so it is often used in modelling when the effects of several simultaneous reactions are approximated with just one kinetic reaction.

Friedman [40] presented several equations for calculation of N. The following equation is based on three well-separated reference points from the same data

$$N = \frac{\ln\left(\frac{(\frac{d\alpha}{dT})_3}{(\frac{d\alpha}{dT})_1}\right) - \frac{T_2(T_3-T_1)}{T_3(T_2-T_1)} \cdot \ln\left(\frac{(\frac{d\alpha}{dT})_2}{(\frac{d\alpha}{dT})_1}\right)}{\frac{T_2(T_3-T_1)}{T_3(T_2-T_1)} \cdot \ln\left(\frac{1-\alpha_1}{1-\alpha_2}\right) - \ln\left(\frac{1-\alpha_1}{1-\alpha_3}\right)} \tag{2.26}$$

This method works very well for smooth data and non-overlapping reactions but may be complicated for real data, as discussed in Publication II.

Gao [48] has provided a more practical approach by listing theoretical limits for the reaction order as a function of the conversion. Through a polynomial curve fit, those values convert into a very simple relationship (as demonstrated in Publication II):

$$N \approx 13.25(1-\alpha_p^*)^3 - 4.16(1-\alpha_p^*)^2 + 2.3(1-\alpha_p^*) - 0.077, \tag{2.27}$$

where α_p^* is the reaction progress variable at the peak of the reaction.

The isoconversional method provides also a good way of defining N. Li and Järvelä [24] suggest that the reaction rate can be expressed as

$$r = \frac{(\frac{d\alpha}{dt})}{(1-\alpha)^N}. \tag{2.28}$$

After one takes a natural logarithm and rearranges this, it results in

$$\ln\left(\frac{d\alpha}{dt}\right) = \ln(r) + N\ln(1-\alpha). \tag{2.29}$$

If $\ln(d\alpha/dt)$ is now plotted against $\ln(1-\alpha)$ at several temperatures, the N value is equal to the average slope of these lines.

2.4.2 Optimization algorithms

The analytical methods solve the parameters by using reference points, and the results depend only on the choice of method and the location of the reference point. Another approach is to consider the parameter estimation as an optimisation problem wherein the model is fitted to the experimental data. Several curve-fitting algorithms have been developed over the years. The traditional gradient methods tend to converge at the closest local minimum (not necessarily the global optimum) and therefore generally do not operate well with this kind of problem. Accordingly, evolutionary algorithms were considered. The first attempts used *genetic algorithms* (GA) [17, 19, 31]. These do operate very efficiently for non-linear problems with a large number of unknown parameters. However, GAs may be utterly inefficient with large estimation boundaries and therefore require several iterations and large sets of candidate solutions. Several other algorithms have been studied and successfully used in estimation of the pyrolysis parameters [49–53]. All of these methods require purpose-specific software and significant computation time, and their stochastic nature means that the estimation procedure cannot be repeated exactly. The results also depend on the estimation boundaries and algorithm parameters defined by the user. However, the above mentioned shortcomings are compensated by the algorithms' advantage of not being limited to any specific model. Besides the pyrolysis kinetics, a GA can be used in estimation of any other parameters. In the fire sciences, these other parameters would typically be the thermal parameters as listed in Table 2.1.

The idea of **GA** [17, 19, 31] is based on the evolution and survival of the fittest. Each set of parameters represents one individual in a population. The individuals consist of parameters – or *genes*, as they are called in GA argot. The first population is selected randomly from the pre-defined range. The individuals are located in several subpopulations that do not share the genes in normal routines. Each individual is tested against the experimental data, and a value called the *fitness value* is calculated for measuring the goodness of the fit. The population goes through a set of operations that are stochastic, and their probabilities depend on the fitness value. These operations include *selection* (selecting the best-fitting solutions for reproduction), *cross-over* (combining two selected individuals for production of a new individual, offspring), *mutation* (changing one or more genes of some individuals into a random number), and *migration* (migrating, on the part of individuals, between subpopulations). The next generation consists of the best fitting individuals of the previous generation and of the new offspring. The operations based on the fitness value and probabilities cause the population converge towards the best fitting solutions,

and the mutation and the migration bring new genes to the subpopulations and hence prevent convergence at a local minimum. A flowchart of the algorithm is shown in Figure 2.7. This topic is further discussed in Subsection 4.4.2 and in Publication I.

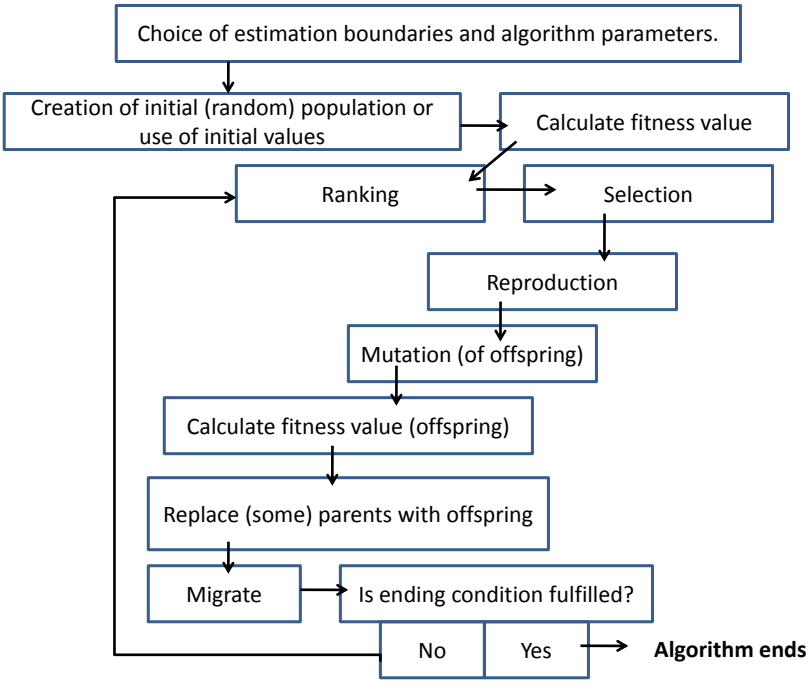

Figure 2.7. Flowchart of a genetic algorithm.

Shuffled complex evolution (SCE) is, in essence, an improved genetic algorithm [49, 54]. It starts similarly, with a random population, but is better organised and optimised with respect to the following operations. First, the individuals are ordered according to their fitness values. Then they are divided into *complexes* such that every nth individual is placed in the same group. Every individual within a complex, a probability then is assigned that determines which q individuals are to be selected for a *subcomplex*. The values are ordered by their fitness values. The worst fitting value (u_q) in the subcomplex is compared to other values within the group and a new value is calculated as

$$r = \frac{2}{1-q} \sum_{j=1}^{1-q} -u_q. \tag{2.30}$$

If r is not within the estimation boundaries, a new random value is generated instead. If the fitness value of the new value is smaller than previously

($f_r < f_q$), the new value r replaces the old value u_q. Otherwise, a new value is calculated, as

$$c = \frac{\frac{1}{1-q}\sum_{j=1}^{q-1} + u_q}{2}. \tag{2.31}$$

Comparison of the fitness values is performed as before. This operation is repeated within the subcomplex until the predetermined number of iterations are completed. After that, the same operations are performed for each of the other subcomplexes. When all the subcomplexes have been gone through, the convergence condition is checked. If this has been satisfied, the algorithm ends. If not, it starts running again from the sorting of the fitness values and distribution of candidate solutions to complexes.

This method has been applied to estimation of the parameters related to thermal degradation of several materials by Chaos et al. [49] and Lautenberger and Fernandez-Pello [50]. The SCE approach has proved to be more efficient and to provide more accurate results than GAs do.

Hybrid genetic algorithms (HGA) combine the evolutionary algorithm and local search methods (e.g., gradient methods) [52, 55–57]. They have been developed to enhance the algorithm such that it produces higher quality solutions more efficiently. The local search method can be included in any of three phases in the estimation process: before, during, or after the algorithm. Before the GA operation (*pre-hybridisation*), the local search is used for generating the initial population for the GA and therefore reducing the solution space. This is suitable for some specific problems but not in general. The second option, which some refer to as *organic hybridization*, is used as one more operator for the GA, improving the fit of each individual in each generation. Although this is computationally more efficient than a GA alone, there is no guarantee of finding the global optimum. The last method is referred to as *post-hybridisation*. Here a GA is used to provide the initial design for the local search method. This has proved to be generally the most efficient way to hybridise the GA, since the global and local searches are performed completely separately.

Saha et al. [52] have successfully applied HGA for estimation of the kinetic parameters of various plastics. They used the post-hybridisation technique and a multidimensional, unconstrained non-linear search function as a hybrid function.

Stochastic hill climber (SHC) algorithm was developed by Webster [53] for his master's thesis in 2009. The algorithm differs from GAs in the following respects:

- The initial population is generated via good engineering judgement (or by rules of thumb, discussed in Subsection 4.4.3). Webster has stated that it

is more logical to start with a well-fitting curve that has 'wrong' parameters than with a non-fitting curve that has the 'right' parameters.
- The fitness function involves an R-squared value.
- Reproduction is done via mutation only (i.e. with no cross-breeding). The parents may outlive the children if they have better fit.
- The mutation magnitude of each parameter is limited such that each can effect no more than 5% change in accuracy. This is done in order to prevent any single parameter from dominating in the estimation process.
- The mutation magnitude is multiplied by a scalar that depends on the mutation history of the parameter. If the previous mutation attempts have been successful, the scalar has a higher value than if the mutations have been unsuccessful.

This method has been applied to the estimation of cone calorimeter results by Webster himself, and by Lautenberger and Fernandez-Pello [50], with good results.

Simulated annealing (SA) differs from the previously presented algorithms in not being an evolutionary algorithm. It is, however, based on a real-life process – namely, annealing in metallurgy. In annealing, the material is first heated and then cooled, for finding of lower internal energies. In the algorithm, the initial solution is tested against a random solution. The choice of solution is based on the difference in fits and a random number that depends on a parameter referred to as *temperature*. The temperature is eventually decreased, and the probability of choosing the worse-fitting solution decreases with it [51, 58, 59]. Mani et al. [51] applied SA for estimating the kinetic parameters of lignin with good results.

Lautenberger and Fernandez-Pello [50] compared the performance of four algorithms (a GA, SCE, SHC, and a hybrid of a GA and SA). They tested these estimation methods by using generic cone calorimeter data, so that the real target values of the parameters were known. They evaluated the algorithms in terms of their effectiveness and robustness. The most rapid convergence was shown by SHC, but the final fitness was at a level similar to that with GA and HGA, and SCE turned out to perform with the best fit with any random initial population. These solutions were practically independent for the initial population, and it seems that SCE is able to find an actual global optimum for the problem. When the target values of the parameters were compared, the values estimated via SCE were the most accurate by far. The other algorithms were much less accurate with respect to correctness of the target values, with HGA producing the greatest accuracy of the three while SHC showed the least accurate fit.

2.4.3 The compensation effect

As is discussed above, the values for the activation energy may be very sensitive to small changes in experimental conditions (such as heating rate); therefore, isoconversional methods are commonly used, preferred over a single heating rate experiments. This phenomenon is also widely recognised in the literature [25, 60, 61] and observed in experiments, but no comprehensive explanation has been provided so far. There are two main, and opposite, points of view on the nature of the compensation effect; it either is caused by an experimental artefact or has a true chemical meaning. The second case is often seen as discomforting, since it means that the A and E values are not independent and therefore do not have any physical meaning in isolation. In fire modelling, the interpretation has been that the compensation effect has a chemical meaning.

The general form of the compensation effect is

$$\ln(A) = a + bE, \tag{2.32}$$

where a can be very small [60, 61]. The analytical form of the compensation effect is, according to Nikolaev et al. [60],

$$\ln(A) = \ln\left(\frac{E\beta}{RT_p^2}\right) + \frac{E}{RT_p}. \tag{2.33}$$

Slightly different form for the compensation effect has been suggested by Lyon and Safronava [62]:

$$\ln(A) = \ln\left(\frac{\beta E}{\phi RT_p^2}\right) + \frac{1}{RT_p}E, \tag{2.34}$$

where $\phi = -df(\alpha)/d\alpha$. The compensation effect depends on rate and model, as observed.

Similar behaviour has been observed more generally with other model parameters, especially with larger-scale models. The models inevitably have some degree of inaccuracy, and the parameters combine to form a model that fits to experiments. Therefore, the model parameters actually work together to compensate for the shortcomings of the model and several combinations, fitting equally well, can be found for the same experimental data. This phenomenon is demonstrated and discussed in Publication III. However, good initial guesses (e.g., by model-free methods) may help to eliminate the randomness of the solutions and keep the parameters more realistic [63].

2.5 The Monte Carlo technique

Fire modelling can be used as a part of PRA. The goal of fire-PRA is to determine the probability of the various possible consequences of a fire and discover the most significant parameters that correlate with the most severe conditions. The *Monte Carlo* (MC) technique is a tool for the statistical assessment. This method is not used for parameter estimation as the methods described previously in Section 2.4. In this dissertation, it has been used to statistically study fire spread from one cable tray to another, as described in Publication V.

The Monte Carlo technique in its simplest form means repeating an action several times at a random points in a parameter space and counting the events. A simple example of this technique is a game of tossing a coin to estimate the probability of heads or tails. The modern Monte Carlo was born in the 1940s when Stanislaw Ulam, John von Neumann, and others, started to use random numbers in the calculations of statistical physics. The most efficient use of the MC technique is to determine definite integrals that are too complex to solve analytically. [64, 65]

In applications of Monte Carlo for fire research, a simulation is repeated several times, using random numbers from certain distributions of input parameters. The number of repetitions should be high enough to cover the variable space for capturing the statistics of the events. This is computationally quite expensive, so a more optimised sampling method is used. The sampling method, called *Latin hypercubes* (LH), is a type of stratified sampling. The idea is to divide the range of each variable into as many intervals as the number of samples so that each interval has equal probability according to the distribution. From each interval, one random number is selected, and the random numbers of each parameter are paired in a random manner. As its result the sample represents the space of possible input values more extensively than traditional random sampling does, and, therefore, fewer repetitions are required. [66, 67]

For fire Monte Carlo, a software package called Probabilistic Fire Simulator (PFS) is used. It was developed at VTT Technical Research Centre of Finland. It runs Monte Carlo (or two-model Monte Carlo) with a chosen fire model, most commonly with FDS [68, 69]. This tool has been used in the simulations described in Publication V.

3. Materials

3.1 Motivation

The thermal degradation process depends on the material. The degradation varies with the polymer classes, whether the surface swells or shrinks when heated and what kinds of flame retardants, if any, are used. A brief literature survey is presented that considers these processes. Special attention is given to complex but very important materials: cables and composites. The challenges and the solutions from a modelling point of view are discussed in Section 3.5.

3.2 Thermoset and thermoplastic polymers

Synthetic polymers are classified as *thermoplastic* or *thermoset* by their behaviour when heated. When exposed to heat, thermoplastic polymers soften and melt, and they take a new form when cooled down. This may affect their burning through forming of falling droplets or burning liquid pools. Thermoset polymers, on the other hand, are cross-linked structures that do not melt when heated; they often leave residual char. Of the natural polymers, cellulose is similar in fire behaviour compared to synthetic thermoplastic polymers. A third polymer class would be the elastomers, which can be distinguished by their rubber-like properties. They can behave either like thermosets or as thermoplastics do, depending on the material. [14, 70]

3.3 Modelling shrinking and swelling surfaces

A solid surface seldom maintains its structure when exposed to heat. If a homogeneous material is converted completely to volatiles, the material thickness decreases as the fire progresses. However, many materials do not degrade completely and instead leave empty spaces (*porosity*) in the structure. Some gas from the pores may get trapped under the surface, causing the material to swell. This mechanism acts as a natural flame retardant for many charring materials, and the idea has been adopted for several synthetic flame retardants as well. More about the swelling (or intumescent) surfaces as a flame retardancy mechanism is explained in Section 3.4. Many charring materials (e.g., wood) first swell in the charring phase, and later shrink (in the presence of oxygen) when the char oxidises.

Shrinking and swelling have a significant effect on the thermal degrada-

tion of a material. Increasing porosity decreases the thermal conductivity, and a swollen surface forms a physical barrier to the heat. The simplest way to model this is to calculate the final thickness by using the information about residue fraction and final density. One can calculate the density that the material would have after the reaction if the thickness were to remain unchanged ($\rho_{s,i}$). If the final density (ρ_i) is defined to be higher than the one calculated, the material shrinks; if lower, the material swells. In FDS version 6 [71], this is done by decreasing or increasing the solid cell size in keeping with the ratio of the densities:

$$\delta = \begin{cases} \max_i \left(\frac{\rho_{s,i}}{\rho_i}\right) & \text{if } \max_i \left(\frac{\rho_{s,i}}{\rho_i}\right) \geq 1 \\ \sum_i \left(\frac{\rho_{s,i}}{\rho_i}\right) & \text{if } \max_i \left(\frac{\rho_{s,i}}{\rho_i}\right) < 1. \end{cases} \tag{3.1}$$

The cell thickness is then scaled by this factor, with the thickness from the last time step ($t-1$):

$$\Delta x(t) = \delta \Delta x(t-1), \tag{3.2}$$

and the density similarly:

$$\rho(t) = \frac{\rho(t-1)}{\delta}. \tag{3.3}$$

With this method, it is possible to model the known density or thickness change effectively by manually adjusting the thermal conductivity of the residue to be lower, but the method cannot predict the final thickness. To be able to predict the swelling or shrinking, one must model the porosity. This effort seems at the moment to be overly time consuming when compared to the benefits; therefore, the porosity model has not been included in FDS. However, Zhang et al. [8] developed a model that is able to predict the final thickness. The model takes into account the proportion of the gases that stay trapped under the surface and the conduction in the pores caused by radiation and convection.

The effect of the swelling and shrinking with FDS6 modelling is usefully demonstrated with an example. A charring material with a thickness of $2\,$cm and an initial density of $1,000\,$kg/m^3 degrades ($A = 1 \cdot 10^{10}$ s^{-1}, $E = 1 \cdot 10^5$ kJ/kmol, $N = 1$) yielding a mass fraction of 0.5 fuel gas and 0.5 residue. The thermal conductivity of the residue is $0.05\,$W/(m·K) and the surface area is assumed to remain constant. Comparison of the cone calorimeter simulations is shown in Figure 3.1. It can be seen that, although the thermal degradation process remains the same across all cases (except with swelling or shrinking), the pyrolysis and combustion are faster for the shrinking material. It also has the highest heat release rate peak, a consequence of a shorter period of releasing the same amount of heat (see the first pane in Figure 3.1). The swollen surface

also insulates the surface significantly better, as can be seen from the back-side temperatures (Figure 3.1 pane c).

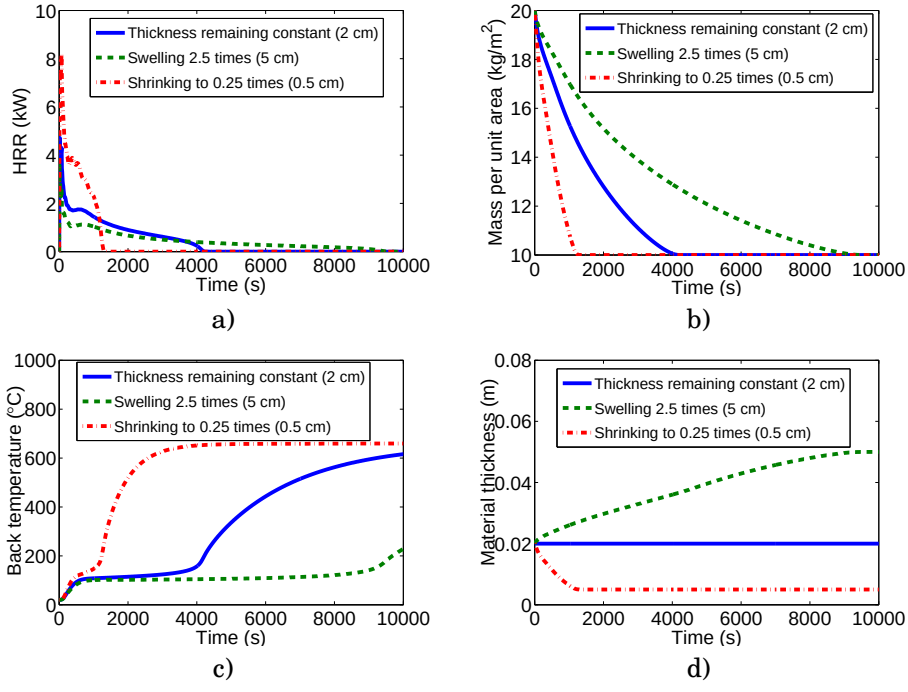

Figure 3.1. The effect of shrinking and swelling surfaces in the cone calorimeter simulations: a) heat release rate, b) mass per unit area, c) back temperature, d) thickness.

3.4 Flame retardant mechanisms

Not all fires can be prevented, but the consequences can be minimised. Several flame retardancy mechanisms have been developed for slowing down the fire spread. This section concentrates on polymers, because of their significant involvement in the fire spread, but similar methods have been used to protect other targets from the heat, such as metal structures, too (e.g., use of intumescent paints).

Use of flame retardant additives does not make the combustible material non-combustible, but it does delay the ignition and/or reduces the heat release rate in the fire. The increased time to react may be significant for the safety of the people and property involved. The choosing of flame retardant or whether one is to be used at all is not trivial. Some flame retardants have the desired effect only in quantities potentially large enough to change the mechanical properties of the polymer. Some flame retardants increase the production of smoke,

which decreases visibility in the event of fire and produces toxic gases. Therefore, the specific needs of each application have to be considered carefully. [6,72]

The flame retardants operate at many levels, in the gas or solid phase, or both. Fire spread is often described as a cycle that starts with pyrolysis in the solid phase (a) that releases flammable volatiles and that in the presence of oxygen (b) leads to flames (c). This, in turn, produces heat (d) that accelerates the pyrolysis. The flaming also may produce smoke and gas species that could be harmful to people. At the first step in the cycle (a), the goal is to affect the pyrolysis reaction in the solid phase. The reaction is modified such that char formation is promoted instead of flammable volatiles. Additionally, the char layer is a good insulator and acts as a barrier between flame and polymer. The second step (b) is to prevent the supply of oxygen to the flame and hence prevent the combustion of volatiles. This can be done via inert gases that are released during pyrolysis. By adding flame inhibiting agents to the polymer that are released near polymer degradation temperature, one can exert an effect on the flame directly (c). The last step in the cycle is to prevent heat flow back to the polymer (d). This can be done by means of either a heat sink that degrades endothermically or a physical barrier such as char or an intumescent coating. Naturally, many flame retardants act at multiple points in the fire cycle. [6,72]

At the pyrolysis stage (a) and for preventing the feedback from the flames (d), char formation is the most important mechanism for retarding the flame. Char forms an insulating barrier at the surface which delays the heat conduction to the polymer. An increased proportion of char also contributes to fewer flammable volatiles being released during pyrolysis. Significant amounts of flame retardant agents are added to the polymer, and these interact at temperatures lower than that of the polymer pyrolysis. There are two main methods by which polymers may promote char formation: dehydration and cross-linking. Dehydration is commonly associated with phosphorus derived compounds and the decreasing oxygen content in the polymer. Cross-linking stabilises the polymer by providing additional, strong bonds to the polymer chain. It has been suggested also that cross-linking increases the viscosity of the molten polymer that contributes to retarding the flow of the volatiles to the flame.

Cellulose is a good example of these mechanisms. With addition of only 2% phosphorus, the cellulose polymer is fire protected through dehydration process. It also cross-links at elevated temperatures, forming char. Nanocomposites are another example of flame retarding by char formation, more specifically by formation of high-performance carbonaceous-silicate char. Composites are discussed in greated depth in Subsection 3.5.3. [6,73]

Intumescent surfaces insulate the polymer surface with a porous, carbonaceous layer of char. The mechanism should not be confused with the char-

ring process. For an intumescent coating to form, three active components are needed: acid source, blowing agent, and charring agent. The acid source breaks down, forming a mineral acid that acts as a catalyst. This participates in the charring reaction together with the charring agent. The blowing agent produces large amounts of gaseous products that remain partly trapped under the surface, making the surface swell. [6, 8]

Another way to protect the polymer in the solid phase is to cool it down with an *endothermic* (energy-requiring) reaction. Hydrated minerals (the most commonly used are *alumina trihydrate* ($Al(OH)_3$, ATH) and *magnesium hydroxide* ($Mg(OH)_2$, MDH)) act this way, releasing water. The water also dilutes the pyrolysis gas and decreases the concentration of the flammable gas. The water content of ATH is 35% and that of MDH 31%. Their degradation temperatures and enthalpies as given in the literature vary slightly and are listed in Table 3.1. While MDH is more attractive in many applications for its higher degradation temperature and higher enthalpy, in practise ATH has been more commonly used, on account of its the lower price. [6, 7]

Table 3.1. Values in the literature for decomposition temperature and enthalpy for ATH and MDH (enthalpy is reported as required energy, positive endothermic reaction values).

	ATH		MDH	
In reference	T (°C)	ΔH (kJ/kg)	T (°C)	ΔH (kJ/kg)
[7]	180–200	1300	300–320	1450
[6]	205	1172	320	1598
[73, 74]	220	1170	330	1356

The oxygen concentration near the flame (b) can be reduced via release of an inert gas, as water or chlorides, in the gas phase, in a mechanism similar to that seen with the mineral fillers discussed earlier.

In gas phase (c), the halogens are the most prevalent group of flame inhibitors, especially chlorine and bromine. The free radicals $H\cdot$ and $OH\cdot$ have an important role in the process leading to thermal degradation and combustion. Halogens are known to react rapidly with these radicals and produce compounds that are much less active and therefore inhibit the flame. For example, PVC is flame retardant on account of its chlorine (more specifically, *hydrochloric acid*, HCl). The flame retarding effect of halogens is considerably less with large and hot fires, because the equilibrium of the halogen molecules decreases at increased temperatures. Some phosphorus chemicals are known to have similar effects in the gas phase, although they also act in the solid phase, via glass formation. [6, 14, 73, 75]

There has been much discussion about the disadvantages of the halogenated

flame retardants, mostly those containing *diphenyl oxide* (DPO), due to the toxic fumes they release during fire. At the other extreme, completely avoiding flame retardants increases the number of fires and therefore also the amount of toxic smoke. [75] The current trend is toward abandoning halogenated flame retardants because better alternatives have been developed.

3.5 Complex materials for fire modelling

The typical materials involved in fires (and fire simulations) seldom are fully characterised in their properties, homogeneous in structure, and of simple geometry, as a *poly(methyl methacrylate)* (PMMA) sheet is. In contrast, they take part in several chemical reactions and processes, contain additives, and have layered structures and complex geometry. Often the exact compound of the material is a business secret and therefore not publicly available knowledge. All of this makes the fire modelling of these materials challenging. This section of the thesis presents some of the typical applications of fire modelling. The materials and structures are reviewed from the standpoint of modelling of the fire spread.

3.5.1 PVC and its additives

A thermoplastic material with a wide range of applications, PVC is used in pipes and cables, as well as in clothes, furniture and sport equipment. Electrical cables are one of the most interesting applications from the point of view of fire modelling, since they constitute a significant fire risk at power plants and other facilities with lots of electronics. Pure PVC (C_2H_3Cl) is rigid, but often applications utilise PVC in its plasticised form ($C_{26}H_{39}O_2Cl$). Besides plasticisers, PVC material may include other additives, such as stabilisers and fillers. Rigid PVC burns, yielding char, only when an external heat source is present. If the heat source is removed, PVC extinguishes immediately. Plasticised PVC burns much better, because of the plasticisers' high heat of combustion. As is discussed in Section 3.4, PVC is inherently flame retardant, on account of the release of inert, diluting gas (HCl), and char forming. HCl is highly corrosive and therefore poses a hazard to people and property. [6, 70]

PVC has been widely studied experimentally [76–83] and in numerical analysis [81, 82, 84–87]. The degradation of pure PVC occurs in two steps. The first of these (at around 200–300°C) is dominated by a process that mainly releases HCl and hence is called dehydrochlorination. This non-combustible compound dilutes the gas phase and promotes char formation at the surface. The remaining polyene structure starts degrading immediately after this, releasing small amounts of aromatic hydrocarbons, mainly benzene ($\Delta H_c = 40$ MJ/kg [14]).

The stoichiometric amount of HCl released in PVC is 58.7%, on the assumption that all chlorine is released as HCl during the first step in the degradation. According to thermogravimetric studies performed by Miranda et al. [82] in vacuum and nitrogen, the mass loss from the first reaction is 64% and the remaining chlorine 0.14% at a 10 K/min heating rate. This process is not very sensitive to heating rate or environment (vacuum or nitrogen). The excess mass loss in the first reaction (5.44%) is identified as release of aromatics. The second major mass loss occurs at around 450°C, releasing toluene and other alkyl aromatics. The mass loss from the second reaction depends on the heating rate and environment. In Miranda et al. studies, the residue content varied (at heating rates of 1–20 K/min) from 3.1% to 6.4% in vacuum and over the range 6.9–12.4% in nitrogen. This leaves an average of 31% in vacuum and 26% in nitrogen for the second reaction mass loss. The residue content increases with the heating rate and is lower in vacuum than in normal atmospheric pressure. Naturally, the residue content in air is lower than in nitrogen, because of the oxidative effect, as can be seen in the TGA results for almost pure PVC pipe material that are presented in Figure 3.2. [6, 77, 82]

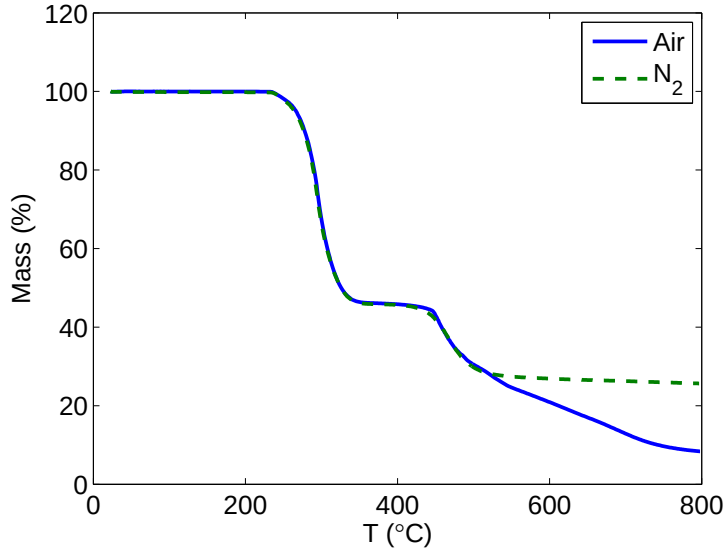

Figure 3.2. TGA experiment of almost pure PVC pipe material at 10 K/min.

What makes PVC a complex subject of modelling are the additives. In many applications (e.g., electrical cables) PVC is used in its flexible form, in which the pure PVC is mixed with plasticisers in significant amounts. Besides plasticisers, a PVC cable may include stabilisers and fillers, which affect the thermal degradation and combustion.

The most important additive from angle of the fire spread is the plasticiser, concentrations of which can be as high as 100 phr (parts per hundred parts resin). There are several commercial plasticisers available, of which one of the most commonly studied (and used) is *diethylhexyl phthalate* (DOP). The phthalates degrade at around the temperature at which the dehydrochlorination reaction occurs and releases combustible gases that burn with a flame in the presence of oxygen. Besides increasing the fire risk through the mechanism of flammable gas, plasticisers interact with the PVC resin and alter the thermal degradation process. Marcilla and Beltran [81] studied pure samples of DOP and PVC and their mixtures in TGA. The degradation temperatures of these two components are slightly different; DOP degrades at slightly lower temperatures than pure PVC. In a mixture, the temperatures almost overlap; the degradation temperature of DOP increases only slightly, but the PVC degrades clearly earlier than it does without plasticisers. The low concentrations of plasticiser and high heating rates decrease the effect. Similar destabilisation of the PVC was observed by Jimenez et al. [79]. They provided two explanations for the phenomenon: As the DOP evaporates, it leaves holes in the resin structure that act as the starting points of the HCl release. Another cause may be the reaction accelerating radicals formed at around $300\,^{\circ}\mathrm{C}$ as the DOP evaporates. Additionally, it was observed that DOP partially inhibits the formation of aromatics during the dehydrochlorination reaction.

The most significant additives in PVC mixtures, by concentration, are fillers. Reasons for the use of fillers range from improving the flame resistance (via minerals ATH and MDH), thermal stability (via calcium carbonate, $CaCO_3$), and electrical (via metal and carbon fibres) and mechanical (for example, via talc) properties to simply cost reduction. In PVC cables, the most common filler is $CaCO_3$. [88] It degrades at high temperatures, producing CO_2 and H_2O. It may also react with HCl to produce calsium chloride (CaCl). [89, 90]

Other significant groups of additives are stabilisers and metal oxides. They are not added in large quantities but do have an effect on the thermal degradation of the polymer. Stabilisers do not directly affect the degradation temperatures, but they do inhibit the formation of HCl, which is an important result from the environmental point of view. At higher concentrations (> 1 phr), these stabilisers also inhibit the benzene and toluene formation, thus decreasing the amount of combustible gases. [79] The metal oxides also suppress the formation of aromatics, for unsubstituted aromatics (benzene, and naphthalene), the effect being more significant than for alkyl-aromatics (toluene). The oxides with the greatest aromatic suppression effect also promote char formation the most. Some metal oxides (mainly ZnO) also lower the dehydrochlorination temperature. [77]

3.5.2 Electrical cables

Fire is considered one of the initial events to be examined in PRA for nuclear power plants. Electrical cables account for a significant portion of their fire load, and so cable fires have been widely studied both nationally [4] and internationally [91]. The fire itself is not the only hazard in those applications; also, failure of critical instrumentation or control cables may lead to severe consequences.

Early on cable modelling concentrated on simple, analytical models and approximations [92, 93]. With advances in processing power and CFD code, actual prediction of the fire spread, starting with the material reactions, has become more feasible. The dissertation project concentrated on the new methods for modelling cable fires more accurately.

As was noted earlier in this chapter, obtaining information about cable composition may be challenging on account of lack of information. Some cables in a nuclear power plant may have been installed decades ago and leave no way of identifying the cable composition except through extensive analysis of each cable individually. It is fortuitous that knowing the exact compound does not seem to be as critical for the modelling as it is to be able to predict the effective behaviour of the material. The small scale experiments (TGA, DSC, and possibly MCC) in combination with a bench scale experiment (use of a cone calorimeter) provide enough information for building of an accurate model.

With cables, the geometry and structure pose the biggest challenges. The cylindrical, non-uniform structure of a cable is impossible to model exactly via CFD code, in consequence of the limitations of the grid and material definitions. It is important to understand that the model is not, and does not need to be, an imitation of the reality in full; it is an approximation in which all the parameters taken together compensate for the shortcomings and uncertainties of the model (see Subsection 2.4.3).

Therefore, there are alternative ways to model a cylindrical, non-uniform object. The simplest way is to project the cylindrical geometry to Cartesian coordinates, modelling the cables as rectangular blocks. In this case, the large scale model is limited for the gas phase grid by the dimensions.

An alternative method, still under development, is to use sub-grid-scale (SGS) objects (in FDS, called Lagrangian particles) [43]. In SGS the particles behave equivalently to water droplets, but they may have surface properties of solid blocks. For particles, using a cylindrical form is feasible, and, therefore, the geometry can be interpreted more accurately. The challenges with the particles are related to radiation, flow drag and increased computation time.

The non-uniform layered structure is even more difficult to address. Since most cables do not have separate layers neatly ordered from the surface to core,

one has to approximate this too. Fortunately, other modelling parameters compensate also for this inaccuracy. The sheath layer is always on the exterior boundaries, first and last layers in the Cartesian, only the first in the cylindrical. The rest of the layers can be combined in accordance with the modeller's preferences. For example, the insulation and filler components may be taken in combination as a homogeneous layer, and the conductor may or may not be included in the model, since it does not degrade. An example of a cable model in two geometries is shown in Figure 3.3. It could be argued, that the non-combustible metal conductor needs to be included, since it operates as a heat sink and therefore participates in the process of thermal degradation, but this effect can be modelled through suitable adjustment of the thermal parameters of the other layers. In many large scale calculations, pyrolysis calculations for the solid obstacles are relatively time consuming, so it may be beneficial in those cases to keep the model as simple and thin as possible. However, all the degrading components should still be included, and with use of their actual mass fractions.

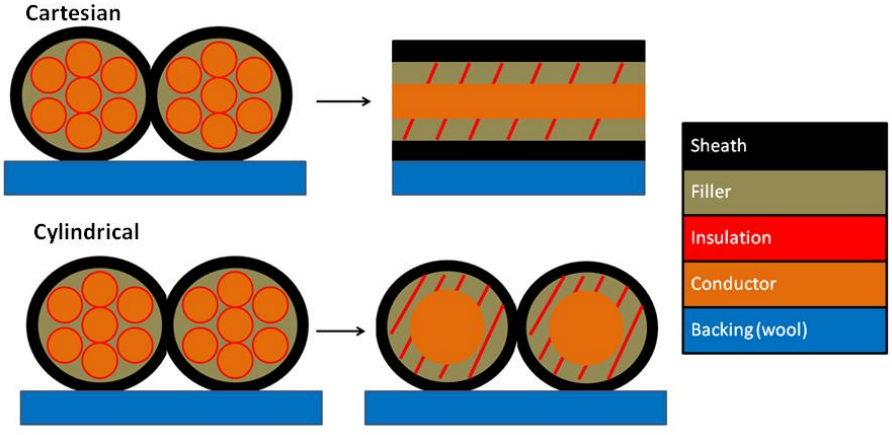

Figure 3.3. Examples of approximation of cable structure in Cartesian and cylindrical geometries.

Often in the NPP applications, it is important to know whether or not the cable can continue operating. Several models have been developed for calculating this [94, 95]. It has been shown experimentally that most PVC cables fail when the temperature within the cable exceeds 200°C. [94]

Since the cables lie in their cable tunnels for decades in varying conditions, it have to be considered that their properties may change. The important question is whether this increases the flammability of the cables. Some experimental studies have been performed that compare new and old PVC cables, and

it seems that the time of ignition is actually longer with old cables. The explanation may have to do with slow evaporation of the phthalates, leaving less combustible material in the cable. [96,97] Another question is how the evaporation influence the cable's mechanical properties. Placek and Kohout [98] studied PVC-sheathed cables after exposing them to radiation and high temperatures, corresponding to 10 years of real-world service. They noticed that mechanical properties (strength and elongation) in the sheath area were not significantly inferior to those of the new sample. However, in the insulation the effects were more significant, especially with slow ageing. These effects were connected with oxygen diffusion causing extensive degradation. The model for calculating the time of simulated ageing has been presented by Benes et al. [83].

3.5.3 Composites

Composites are made of two or more materials that are united through artificial combinations. The artificial fabrication is an important feature differentiating composites from, for example, metal alloys. Composites have the advantage of combining properties of two or more materials and therefore have qualities that individual components cannot attain alone. They can be tailored in many ways through careful choice of the components and their proportions, the distributions, morphologies, degrees of crystallinity, crystallographic texture, structure, and the composition of the interface between the components. Composites combining suitable qualities in these categories can be lightweight, stiff, strong, resistant to corrosion, durable, and thermally isolating, and they can have low thermal expansion, among other characteristics. [99, 100]

The idea behind composites is not new. The first known composites were developed by the ancient Egyptians when they reinforced their mud and clay bricks with straw and developed the first version of plywood by combining many thin layers of wood into one thick layer [101]. Composites were used in the construction of the Great Wall of China (starting in 121 BC) too, where earth-works were connected and reinforced with bricks that included, along with water and fine gravel, red willow reeds and twigs. In Mongolia, bows were made via lamination of animal horns and tendons, wood, or silk around 1200 AD [102]

Since those days, civil engineers and designers have striven to develop new forms of materials for stronger, larger, better, and more aesthetically pleasing structures. Since the 1960s, the use of polymer composites has grown very rapidly. Composites are used in applications from aircraft and race cars to sporting goods and consumer products. [101, 103, 104] Biodegradable and lignocellulosic fibre composites have been developed since the 1990s, because of the growing interest in eco-friendly materials and increased prices of oil [102].

Some challenges with composites are related to their mechanical properties, low through-thickness, poor toleration of impact damage, and anisotropic properties. One major disadvantage is their poor performance in fire. Some composite matrixes soften, creep, and distort already at relatively low temperatures (> 100–$200°$C), which can lead to problems with load-bearing installations. Organic fibres used to reinforce the composite also decompose in higher temperatures (300–$400°$C), releasing fuel gases, which leads to fire in the presence of oxygen. The consequences of this fire include heat, smoke, and toxic gases. The fire products with combination with the decreasing structural durability make the fire behaviour of this type of composites extremely dangerous. [100]

Composites are seeing increasing use in the aeronautical industry thanks to their low density and their strength, along with the possibility they present for optimising the design to achieve the best strength–weight and stiffness–weight ratios. In aeroplanes, the high flammability of composites causes a huge risk, since evacuation possibilities are limited. In 1987–1996, only 3.5% of accidents on aeroplanes originated through fire. Although the number of the accidents was small, they had the fourth largest contribution to the total casualties of all accidents, causing 339 deaths over that nine-year period. Most accidents related to fire on the aeroplanes originate from outside from a fuel tank explosion. In those cases, the integrity and thermal resistance of the cabin are fundamental for the survival of the passengers. Composites display high thermal stability and slow conduction of heat through the thickness; therefore, they are more suitable for use as thermal barriers than, e.g., metal alloys. The high flammability of the composites can be improved by various mechanisms, including heat sinks, heat barriers and fillers that act in the solid or gas phase, in various ways. [2, 7, 100, 105–107]

Research and modelling of the thermal behaviour of fibre-reinforced polymer composites had its beginnings in tandem with the defence and aerospace industries' concentration on carbon fibre materials. The first person to model mechanical properties at elevated temperatures was Springer, who did so in 1984 [108]. He related the mechanical properties empirically to mass loss. Since then, the models have improved greatly, especially in terms of elastic and viscoelastic behaviour at elevated or high temperatures. Bai and Keller [109] provide a good overview of the thermomechanical models developed thus far.

The modelling of thermal degradation of flame retardant polymer composites has been widely studied in the past few years. In 2000, Dembsey and Jacoby [110] studied ignition models for marine cored composites and concluded that the ignition models in use at the time were not able to predict the effect of skin thickness and core composition. A good compilation of analytical models for composites in various circumstances has been presented by Lattimer

and Cambell [111]. A common trend in recent years has been to model the thermal degradation of the materials by using Arrhenius-type kinetics with the three generally unknown parameters per reaction that are as discussed in Section 2.2. This approach has been successfully applied for composite materials by Kim et al. [112] and by Lautenberger et al. [113]. Trelles and Lattimer [114] have suggested an alternative model that is based on the relationship between density and temperature. That model shows good agreement with the experimental data.

4. Methods

4.1 Motivation

This chapter presents methods and applications developed during the work for this dissertation. These methods have been applied and described in detail in the Publications I-V. First is discussion of the parameter estimation process, presenting the best practise and all of the experiences collected during the modelling work, from the sample preparation all the way to the model validation on large scale. The following sections present methods for the individual phases of the modelling process. The FDS models for the experiments are briefly described, as are the parameter estimation methods used in this work. Finally, the method of combining TGA and MCC results is reviewed in brief.

4.2 The parameter estimation process

This section presents the best practise and observations gathered over the years of working with parameter estimation for various materials. A summary of the process is shown in Figure 4.1. It consists of four phases: sample preparation, experimental work, modelling and parameter estimation, and model validation.

The sample preparation is the preliminary phase to the experimental work. If the sample is not homogeneous and has several separable components, each component should be tested separately in the TGA. Therefore, the first step is to deconstruct the material. Some non-homogeneous materials cannot be deconstructed as easily, one example being fibre reinforced composites. In their case, it would be best to test the resin separately from the fibres. If the materials are not available in pure form, small solid cubic forms will work better than a powder made of the sample. The decomposition energies change due to forming of powder, which lead to different results. Also, powder does not necessarily have the same component mass fraction as the original sample, so the results may vary for that reason as well. When the components have been separated, densities and component mass fractions can be determined. At this point it is also necessary to study background information about the sample material. Relevant information would be what the typical additives are, what kinds of reactions should be expected, and so on.

The experimental work includes all of the small and bench scale experiments. The TGA and DSC experiments are performed both in nitrogen and in air, ideally at several heating rates. The maximum temperature should be

set high enough that all the reactions end before the test is complete. A similar principle holds for optional MCC results; if the reactions seem not to have ended when the test ends, or the oxygen content in the combustion chamber indicates that the material consumes all available oxygen, the test should be run again, with adjusted values. Cone calorimeter experiments should be done at least at one heat flux, but results at other heat fluxes are very useful for model validation purposes. Several, identical experiments should be conducted for determination of the experimental error. The experiment should run until the flame extinguishes completely, not only to 20 minutes as the cone calorimeter standard states. The useful measurements are the mass and heat release rate, but in some cases also front and back temperatures of the sample are helpful. An oxygen controlled cone calorimeter can be used for validating the solid phase degradation at the bench scale. The sample's preparation is a complex task, especially for cables. Ideally, each component should be tested separately also on cone calorimeter scale, but, except for the largest cables, the small size and the geometry of the cable components render this impossible. Therefore, cables are usually tested in cone calorimeter in whole form. The sample consist of several parallel 10 centimetre-long cables. The number of cables in a sample depends on their diameter; each sample is approximately $10\,\mathrm{cm}$ wide. The ends of the cables should be wrapped carefully with aluminium foil to prevent ignition from the sides (insulation or filler).

Modelling and parameter estimation is the most important phase in the whole process. It starts with determination of the reaction paths and kinetics for each component separately. The results of TGA and DSC are used for determining the number of reactions, and the results of MCC can be used in measurement of the reaction specific heats of combustion as explained in Section 4.5. The kinetic parameters are estimated from the TGA data. If the fit is acceptable, these values may be fixed in the subsequent steps. At this point, other measured properties (e.g., specific heat, reaction enthalpy, or heat of combustion) are fixed. These measurements are not mandatory, as the parameters can be also estimated from the cone calorimeter results. However, the measurements decrease the possibility of the parameter compensation and help to keep the model more realistic. The cone calorimeter model of any material can be made in several ways, as explained in Subsection 4.3.2. For cables and composites, the layered structure and geometry may not be trivial to model. When the model is chosen, the remaining parameters are estimated by fitting of the model to the experiment. If the fit is not acceptable, it may be reasonable to reconsider the cone calorimeter modelling choices.

Model validation as the final step is an important but often neglected. In its simplest form, it means comparing calculated and measured cone calorimeter

results at multiple heat fluxes that were are not used in the parameter estimation. The model should predict other heat fluxes at acceptable accuracy. At larger scale, validation is even rarer, since large scale experiments are not very commonplace. This is a very important part of the associated software development.

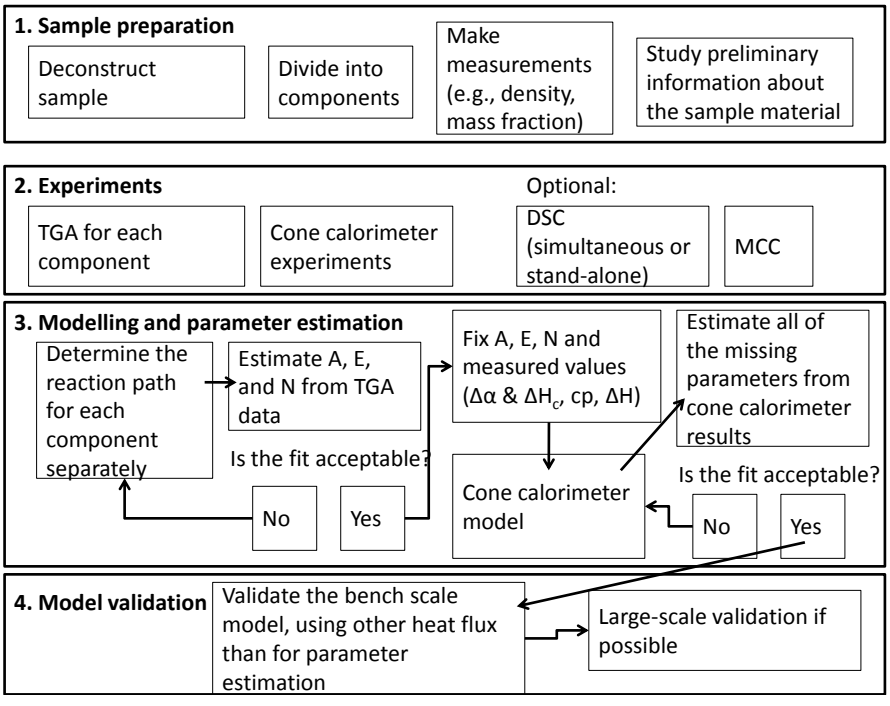

Figure 4.1. The material parameter estimation process.

4.3 FDS models of experimental methods

4.3.1 TGA and MCC

The TGA experiment is modelled for determination of the kinetics of the degradation reaction. The TGA model consists of a relatively large domain (4 m $\times$ 1 m $\times$ 1 m) and coarse grid (25 cm in the z-direction). The physical dimensions do not correspond to the real ones (the real sample cup has a volume of approximately $40\,\mu$l), but, since only the solid phase is being solved, the numerical solution is much more stable with larger dimensions than the actual sample size. Since only the pyrolysis information is desired here, the gas phase calculations are

'turned off' by setting of the ambient oxygen level to be very low. The sample is very thin (0.01 mm) and has a surface of 1 m $\times$ 1 m. The walls around the sample are heated up linearly at the desired heating rate. During the heating, the sample mass and temperature are measured. The sample must be thermally thin enough to be in thermal equilibrium with the heating walls at all times.

An MCC experiment is modelled similar to a TGA experiment for these purposes, only with a higher heating rate (typically around 60 K/min). Since the pyrolysis takes place in inert ambient, only the solid phase is solved. The heat release rate is the result of multiplying the mass loss rate by the heat of complete combustion of the reaction species, which is defined by user.

4.3.2 Cone calorimeter

The cone calorimeter model used in this work consists of two parts: the cone heater and the sample. The sample is either a slab in the bottom of the computational domain or at least one Lagrangian particle over an insulating board. The domain size is 0.3 m $\times 0.3$ m $\times 0.4$ m. The results are somewhat sensitive to the grid size, but 5 or 10 cm has been found to be fast and accurate enough. The resolution of the material model should, naturally, be based also on the final application.

The model of the cone heater depends on the sample model. Traditionally, the heat flux is added directly to the slab-like surface. This is the easiest way because the nominal heat flux of the cone heater at the surface can be determined exactly as in the cone calorimeter. For more complex geometries, especially for the Lagrangian particles, this approach does not work. In those cases, the upper walls are set to high temperatures and thus direct a heat flux to the front surface of the sample. The temperature of the walls depends on the grid cell size and other factors; hence, it should be measured for each set-up separately.

4.4 Estimation methods

The estimation methods discussed here have been developed for, and applied to, the estimation of the pyrolysis parameters. They were used extensively for the research presented in Publications I–V.

4.4.1 The generalized direct method

Various analytical methods used for obtaining the kinetic parameters of pyrolysis reactions were presented in Section 2.4. There are several, quite different approaches, some of them fast and easy to use and others providing very accurate estimates for prediction of the TGA curve. However, most of them are

somehow limited to special cases such as first-order reactions, one reaction step, or only non-noisy experimental data.

It is unfortunate that the real materials are often mixtures of several components; they may take part in multiple reactions, which cannot always be fully separated; and data can be noisy. Hence, a more general approach was developed for Publication II and compared to other known methods.

For generalisation of the method for multiple reactions, a variable for the reaction progress is introduced,

$$\alpha^* = \frac{\alpha - \alpha_{k-1}}{\alpha_k - \alpha_{k-1}}, \tag{4.1}$$

where α_k is the conversion after reaction k. The Arrhenius equation then becomes for multiple reactions

$$\frac{d\alpha}{dT} = \frac{A_k}{\beta} \frac{(\alpha_k - \alpha)_k^N}{\alpha_k - \alpha_{k-1}} exp\left(-\frac{E_k}{RT}\right). \tag{4.2}$$

One reference point can be selected from the peak of the mass gradient. At this reference point, the second derivative is 0 and the mass gradient at the peak is

$$r_{pk} \equiv max\left(\frac{d\alpha}{dT}\right). \tag{4.3}$$

The peak temperature and peak conversion, respectively, are T_p and α_p, correspondingly. From the definition of the peak, the activation energy becomes

$$E_k = N_k R \frac{r_{pk}}{\alpha_k - \alpha_{pk}} T_{pk}^2 = \frac{N_k R}{\beta} \frac{max(d\alpha/dt)}{\alpha_k - \alpha_{pk}} T_{pk}^2, \tag{4.4}$$

depending on whether the derivative is calculated with respect to time or temperature. The pre-exponential factor can be calculated from eq. 4.2 with the activation energy known:

$$A_k = r_{pk} \beta \frac{(\alpha_k - \alpha_{k-1})^{N_k - 1}}{\alpha_k - \alpha_{pk}} exp\left(\frac{E_k}{RT_{pk}}\right). \tag{4.5}$$

This method, which is from here on called *direct method* (DM), is a fast and simple way to define the pair (A_k, E_k), and reaction order can be calculated by means of some of the methods described in Subsection 2.4.1. For this method, only the location of the peak mass gradient and the total mass loss fraction of the reaction need to be known. However, if the reactions partly overlap in temperature (or time), determination of the peak may be challenging. Sometimes there is also more noise at the highest mass loss rate, making the peak value non-exact. For this reason, the idea of the DM is developed further. If the reference point could be selected more freely, e.g., before or after the peak, perhaps

the reaction overlap and possibility of noise would not be a problem. The peak of the second derivative is found from the zero of the third gradient (at T_{pp}). The activation energy then becomes

$$E_k = \frac{-b \pm \sqrt{b^2 - 4ac}}{2a}, where \begin{cases} a = \frac{(\alpha_k - \alpha_{pp})^2}{R^2 T_{pp}^2} \\ b = -\frac{2r_{pp} N_k (\alpha_k - \alpha_{pp})}{R T_{pp}^2} - \frac{2(\alpha_k - \alpha_{pp})^2}{R T_{pp}^3} \\ c = r_{pp}(N_k - 1)N_k - r_{T_{pp}} N_k (\alpha_k - \alpha_{pp}) \end{cases} \tag{4.6}$$

and the pre-exponential factor

$$A_k = r_{ppk} \beta \frac{(\alpha_k - \alpha_{k-1})^{N_k - 1}}{\alpha_k - \alpha_{ppk}} exp\left(\frac{E_k}{R T_{ppk}}\right). \tag{4.7}$$

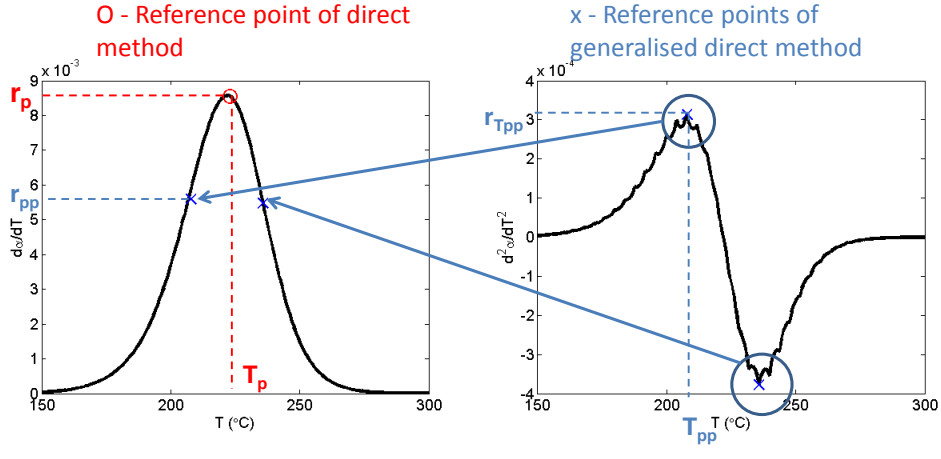

Figure 4.2. Reference points for the direct methods.

This method requires experimental data just at one heating rate. However, because of the compensation effect, several equally fitting (A, E) pairs may be found. Hence, it is important to use several heating rates. In the case of direct methods, the heating rates can be taken into account by averaging of the results (although, Opfermann [115] advise to view this approach with caution). This averaging can be directed to the parameters or to the reference points. Also, the averaging can be weighted for better extrapolation qualities. The alternative methods of weighting are listed in 4.1.

More details and results associated with these methods are provided in Publication II.

Table 4.1. Averaging weights for several heating rates. μ is the mean of the heating rates.

$w_1 = \frac{\mu}{\sum_i \beta_i}$	(direct mean)
$w_2 = \frac{1}{\lvert\beta_i-\mu\rvert \sum_i \frac{1}{\lvert\beta_i-\mu\rvert}}$	(emphasises heating rates near the mean value)
$w_3 = \frac{\lvert\beta_i-\mu\rvert}{\sum_i \lvert\beta_i-\mu\rvert}$	(emphasises heating rates far from the mean value)

4.4.2 Application of genetic algorithms

Sometimes direct methods are not suitable for the parameter estimation, as is discussed in Section 2.4. A GA application was developed for Matlab. The tool is called *PyroPlot*. It uses a free GA toolbox that can be obtained from the University of Sheffield[1]. PyroPlot exploits the toolbox for the algorithm and provides an easy-to-use graphical user interface and an interface to Fire Dynamics Simulator. PyroPlot reads, plots, and filters the data as necessary. It is optimised for the data used in fire simulations, but it can also be applied for other purposes. The GA calculates the model response by using FDS and compares the results to the experimental data. The goodness of the model fit to the experimental results is measured by fitness value. The fitness value is calculated in this application

$$fV = 1 - \sum_k \frac{1}{N_k} \frac{\sum_i (M_{exp,i} - mean(M_{exp}))^2 - (M_{exp,i} - M_{mod,i})^2}{(M_{exp,i} - mean(M_{exp}))^2}, \qquad (4.8)$$

where $\mathrm{M}_{exp,i}$ are the experimental results at each time step i and $\mathrm{M}_{mod,i}$ the corresponding model results. Several results may be compared simultaneously by scaling the fitness value by the number of results N_k. The fitness value is actually the relative error of the model fit, 0 corresponding to perfect fit.

During the simulation, PyroPlot produces plots for the best fitting individuals and indicates the progress of the process in the form of the fitness value. The iteration ends either when the maximum number of generations specified has been reached, or when the user stops it manually because a satisfactory result has been found. Typically, about 50–200 iterations are required with four subpopulations each having 20 individuals. Generating simulated data by using FDS is the bottleneck of the process, but that could be improved through parallel processing. This feature is currently under development.

The accuracy of the results depends on the estimation boundaries and the random numbers used during the process. Relatively wide estimation ranges

[1] See http://www.shef.ac.uk/acse/research/ecrg/getgat

are recommended, for yielding the best possible solution, unless the variable value is known approximately. Because of the stochastic nature of the algorithm, the results are slightly different every time. Especially if there are several solutions, with equal fit (as is typical among TGA results), the solution may converge to very different numbers each time. On occasion an overall fit cannot be found. This may be the case with the cone calorimeter results because of the geometry and layer approximations. In those cases, it is convenient to choose certain parts of the curve (e.g., ignition time and/or the location of the first peak) that have more weight in the fitness value than the other points. This helps the algorithm converge to more acceptable solutions.

PyroPlot can be obtained from Google Code[2] under the MIT License. More information about genetic algorithm and it's application to fire parameter estimation is reported in Publication I.

4.4.3 Sensitivity analysis

Despite of the method used to estimate the model parameters (thermal or kinetic), sometimes there is a need to adjust them manually for obtaining a better fit with the experimental results. In order to do that effectively, understanding of the correlations between model input and the results is required. A sensitivity study was performed for a generic, charring material in the cone calorimeter at $50\,\mathrm{kW/m^2}$ by changing one model parameter at a time. From the results of this sensitivity study, rules of thumb were formulated for summarising the results. These rules are listed in Table 4.2. Definitions for the results are shown in Figure 4.3.

The parameter values were chosen such that the two peaks were well defined. That is not always the case, if the second peak occurs very soon after the first one. The first peak of the two-peaked shape of a charring material comes from the protective char layer building up as a result of the pyrolysis. It increases the thermal resistance between the exposed surface and pyrolysis front, which leads to a decrease in the heat release rate after the maximum is reached. In the cone calorimeter, the back of the sample is often insulated, which prevents heat losses from the back side. Therefore in the end, when the pyrolysis front reaches the back, the heat release rate increases to the second peak. The two peaks overlap in time if the thermal conductivity is high for both the virgin material and residue.

The single most important parameter for all the results turned out to be the activation energy, or the pair ($A,\ E$). The emissivities of both virgin and residue components were also significant in almost all cases. For the ignition

[2] http://code.google.com/p/pyroplot/

time, the other important parameters are thermal conductivity, specific heat, and the absorption coefficient of the virgin material. The time of the first peak is additionally affected by the heat of combustion (in the cases with ambient air). The first peak's height depends also on the heat of reaction of the virgin material, and on the properties of the residue. The time of the second peak and its height depend on all the parameters except the reaction order of the virgin material, and the specific heat of the residue. For flame-out time, all the parameters are significant, apart from the specific heat of the residue.

A similar study has been performed by Stoliarov et al. [116]. They conducted an extensive literature review of the values for several polymers and simulated the model at minimum, maximum, and mean values under several radiant heat fluxes and initial thicknesses. The pyrolysis was modelled by means of the called ThermaKin software, mentioned above. It has a slightly different pyrolysis model than FDS uses. The charring process was not included in the model, but char yield was taken into account. Stoliarov and colleagues studied the variation effects on mass loss rate (MLR), instead of heat release rate. They considered four results: time to mass loss (corresponding to t_{ig}), time to peak MLR (t_{1st_p}), peak MLR (comparable to Q_{1st_p}), and average MLR (not presented in Table 4.2). The results were similar, in view of the differences in the models. For time to ignition, the most important parameter is the ratio A/E. This makes sense, because increasing E and/or decreasing A moves the reaction to higher temperatures. In fact, this ratio turned out to be the most important parameter of all the results studied. Thermal conductivity and specific heat capacity both increase the ignition time, and heat of reaction was found to have no significant effect, in both studies. The differences are in the absorption coefficient and *reflectivity* (defined as $1 - \epsilon$); where the effect is opposite that predicted in the study with FDS (see Table 4.2). For the time of peak, all of the other results are similar except those for the thermal conductivity (positive correlation with FDS and negative in the study of Stoliarov et al.) and reflectivity. The results for the peak height are similar between the two studies (except again for the reflectivity). The differences may be due to the differences in the model, mainly inclusion of the charring reaction in the model.

4.5 MCC methods

Two methods for combining TGA and MCC results have been developed. The first one discussed here is simple and easy to use, while the second is aimed at explaining the material composition more accurately. These methods are presented also in Publication IV.

Table 4.2. Rules of thumb for charring material, where + means a slight increasing, ++ substantial increasing, - slight decreasing and - - substantial decreasing effect in the result, when the particular parameter is increased.

	t_{ig}	t_{1st_p}	Q_{1st_p}	t_{2nd_p}	Q_{2nd_p}	$t_{flameout}$
Virgin material						
A	- -	- -		+	+	-
E	++	++	- -	++	-	++
N						+
k	+	+		- -	+	-
c_p	+	+	-	++	-	+
ΔH			-	+	- -	++
ΔH_c		+	++	-	++	-
κ	+		+	+	-	+
ϵ	++	++	- -	++	-	++
Residue						
k				+	++	- -
c_p			-			

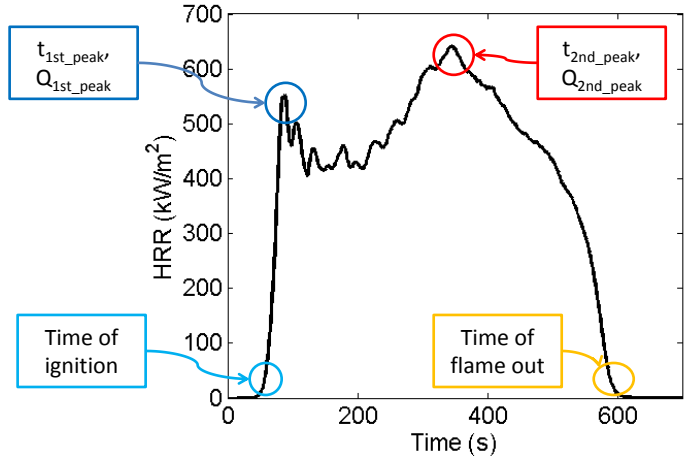

Figure 4.3. Definitions for the rules of thumb.

4.5.1 Method 1

Method 1 could be called an engineering tool. It does not require any information about the material or its composition; it is merely a way of efficiently modelling the correct amount of heat for each reaction. No special software is needed either. A simple reaction path is assumed: Each reaction step cor-

Table 4.3. Input parameters used in generation of the table of rules of thumb.

Parameter (unit)	Baseline		New value
A (s^{-1})	$1{\cdot}10^{18}$	$\rightarrow$	$1{\cdot}10^{17}$
E (J/mol)	$2.5{\cdot}10^{5}$	$\rightarrow$	$2.0{\cdot}10^{5}$
N	2	$\rightarrow$	1
k (virgin and residue) (W/m·K)	0.8	$\rightarrow$	0.4
c_p (virgin) (kJ/kg·K)	2.5	$\rightarrow$	1.8
c_p (residue) (kJ/kg·K)	2.5	$\rightarrow$	1.5
ΔH (kJ/kg)	800	$\rightarrow$	400
ΔH_c (MJ/kg)	40	$\rightarrow$	20
κ (1/m)	50000	$\rightarrow$	500
ϵ	1	$\rightarrow$	0.5

responds to one pseudo-component in the model. Each pseudo-component can yield one fuel and one inert gas. The heat of combustion (ΔH_c) is fixed for all of the reactions. Only the last reaction may yield residue.

The fuel yield ($y_{i,F}$) of each reaction (for all $i < n_r$) can be calculated from

$$y_{i,F} = \frac{Q_i/m_0}{\Delta H_c \Delta\alpha_i}, \tag{4.9}$$

where Q_i/m_0 is the MCC result (heat of complete combustion scaled by initial mass of the sample) and $\Delta\alpha_i$ the relative mass loss of reaction i as observed in TGA. The inert gas yield is thus $y_{i,I} = 1 - y_{i,F}$.

If the material does not yield residue, eq. 4.9 can be used also for the last reaction. If the material does produce residue, the yields of the last reaction become

$$\begin{cases} y_{n_r,F} = \frac{Q_{n_r}/m_0}{\Delta H_c \Delta\alpha_{n_r}}(1 - \frac{Z}{1-\sum_{i=1}^{n_r-1}\Delta\alpha_i}) \\ y_{n_r,I} = (1 - \frac{Q_{n_r}/m_0}{\Delta H_c \Delta\alpha_{n_r}})(1 - \frac{Z}{1-\sum_{i=1}^{n_r-1}\Delta\alpha_i}), \\ y_{n_r,Z} = 1 - y_{n_r,F} - y_{n_r,I} = \frac{Z}{1-\sum_{i=1}^{n_r-1}\Delta\alpha_i} \end{cases} \tag{4.10}$$

where Z is the residue yield of the original mass.

4.5.2 Method 2

Method 2 is intended for the more ambitious modeller who wants to estimate the reaction path and material composition more accurately. The reaction path can be chosen freely, including several parallel, consecutive and even competitive reactions, each yielding several gases and residue. As the reaction path is fixed and can be very complex, there is no analytical way to solve this. There-

fore, the case is constructed as an optimisation problem wherein the objective function is to minimise error between the measured and estimated values. The variables are the initial mass fractions of the components, gas yields and the heat of combustion of each gas. One can include inert gas by setting the heat of combustion to 0. The estimates for the mass loss and energy release of each reaction are

$$\begin{cases} \Delta\hat{\alpha}_i = \sum_{j=1}^{n_c} \sum_{k=1}^{n_{p,j}} y_{i,j,k} Y_{i-1,j} \\ \hat{Q}_i = \sum_{j=1}^{n_c} \sum_{k=1}^{n_{p,j}} y_{i,j,k} Y_{i-1,j} \Delta H_{c,k}, \end{cases} \tag{4.11}$$

where Y_i, j is the mass fraction of component i after reaction j. The calculation is performed recursively from the previous reaction steps;

$$Y_{i,j} = \prod_{ii=1}^{i} y_{ii,j,Z} Y_{i-1,j}. \tag{4.12}$$

The estimation can be performed with using any non-linear solver software, such as, Excel Solver or Matlab Optimization Toolbox. Since the result depends significantly on the initial values, the optimisation is performed through repetition of the process several times with random initial values from the selected range. In this application, the optimisation was made by means of a Matlab function.

4.6 Estimation of the uncertainties

4.6.1 Experimental error

On small scale, the greatest experimental error is related to the sample preparation. The experiments are, in general, highly repeatable if the conditions and the sample are kept identical. This can be seen in Figure 4.4, where the results of repeated MCC experiments are shown for samples of birch wood. The samples were taken from the same board, and some of the board was dried in an oven at $105°$C over a weekend for removal of all moisture. The total heat release of the non-dried wood varies with in the range 11.1–11.2 MJ/kg, with the maximum heat release rate being 164–178 kW/kg and the temperature at the peak between 374 and $376°$C. The heat release rate the dried wood is higher, because the original mass is purely combustible wood. If the results for non-dried wood are scaled in view of the mass of the water (6%), the results look very similar. The difference between the dried material and scaled results is 2.9% for the total heat release, 3% for the peak heat release rate and 0.2% for peak temperature. Although the dried sample is kept in a desiccator, it is quite unclear how

much moisture the dry sample absorbs during the preparations (measurement, sample positioning and heating of the furnace). Therefore, it may be more convenient to test the sample as delivered and determine the moisture content by using another sample.

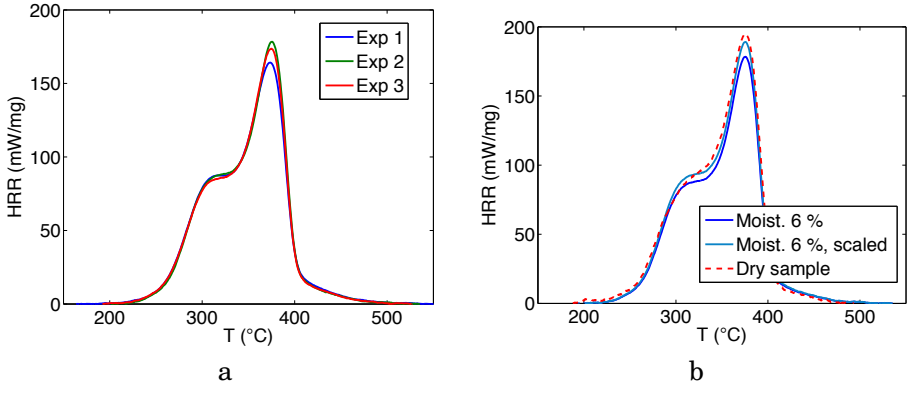

Figure 4.4. Repeated MCC experiments with birch wood. a) non-dried wood, moisture 6% and b) non-dried and dry wood.

The sample mass should be small enough for keeping the sample in thermal equilibrium with the furnace at all times. This is dependent on the thermal thickness of the sample and the heating rate. Also the load cell accuracy is significant with the smallest samples. If the accuracy is 0.1 mg, 10% error could result for the smallest samples.

In the cases involving non-homogenous materials (such as composites), the sample preparation is especially challenging. The material may be very hard to cut, one may be tempted to grate it into powder. In the approach described here, the problem may lie in preserving the sample mass fractions. For example, long fibres may be too big for the sample cup and therefore omitted, leading to lower fibre content and thus greater content of combustibles.

4.6.2 Uncertainties in the modelling

The material model's uncertainty on the larger scale depends on the accuracy of said model and the modelling software. The accuracy of FDS can be evaluated via the verification and validation guides [117, 118]. The verification guide consists of simple examples to verify that the code is implemented correctly, and the validation guide includes a comparison of the experiments and models to confirm that the physics of the several phenomena involved have been handled accurately.

Material model accuracy one the large scale depends on the accuracy of

the small and bench scale model. As is proved in Publication III, it is not the parameter values that are significant on bench scale but the overall fit. The validation work on large scale will continue.

5. Results

5.1 Motivation

This chapter includes summary of the most important results described in Publications I-V and some additional results that shed light on and explain the work done for this dissertation. The estimation methods presented in Publication I and Publication II are compared to other methods in use in terms of accuracy, effectiveness, and ease of use (in Section 5.2). The main results of the sensitivity study performed for Publication III are listed in Section 5.3. Some new results of testing of a PVC cable with the MCC methods developed in the work on Publication IV are reported in Section 5.4, and, a sensitivity study of the cable model used in the large scale MC simulations covered in Publication V is presented in Section 5.5.

5.2 Comparison of estimation methods

The range of estimation methods suitable for extraction of the parameters for pyrolysis models is wide, and often the choice is based on the personal preferences of the modeller. The methods can be divided roughly into two groups, as discussed in Section 2.4: analytical and curve-fitting algorithms. The latter can be applied to any model (including the estimation of thermal parameters), but the analytical methods are model specific. Publication II summarises some commonly used methods for the estimation of kinetic parameters and compares their results' accuracy, their efficiency, and the complexity. The set of methods included two evolutionary algorithms (a *GA* and *SCE*) and four analytical methods, of which one was derived by the author and the others were found in the literature [40, 42, 43]. These methods were tested against two sets of generic experimental data. Generic data were chosen because of the possibility of comparing the real target values to the estimated ones. The first data set was very simple and noiseless, and the reactions were well separated in time. The second data set was more complicated including noise and partly overlapping reactions. Only the analytical methods were tested for data set 2. The interpolation ability of the methods was tested at a heating rate that was within the range of experimental heating rates (20 K/min). The extrapolation ability was tested at a significantly higher rate, 100 K/min. The parameters were also evaluated on larger scale, with the cone calorimeter model and fixed thermal parameters.

The results are summarised in Table 5.1. The reference values were calculated from the generic data. For accuracy of the results, when one considers both fitness values (as in eq.4.8) and difference in the target values, the evolutionary algorithms were superior to the analytical methods. For the former, the user has to define the variable ranges and algorithm parameters. If the algorithm is used with default settings, six lower and upper boundaries have to be determined. For analytical methods, the number of parameters (the complexity) did not correlate directly with the greater accuracy of results. However, the simplest method, the first-order McGrattan-Lyon [42, 43] method, produced the worst fit. The other analytical methods performed well, with good fit in the solutions for both data sets and also for noisy data.

As for their level of accuracy for the end application, all methods tested produce acceptable results. Hence, one can state that the choice of method is basically up to the user.

Table 5.1. Comparison of the estimation methods based on two example cases. Fitness value is the relative error, 0 corresponding to perfect fit. [1]With noise 2. [2]Without parallel computing (algorithms) or automated search for reference values. [3]For algorithms, estimation boundaries etc.

	GA	SCE	DM	GDM	Friedman	McGrattan-Lyon
Fitness value w/ data set 1 (at 100 K/min)	0.0041	0.0003	0.0111	0.0082	0.0109	0.0131
Fitness value w/ data set 2[1] (at 100 K/min)	-	-	0.0143	0.0181	0.0093	0.0553
Time of preparation	10 min	10 min	0 min	0 min	0 min	0 min
Time of estimation[2]	$\approx$ 1 day	$\approx$ 1 day	10 min	15 min	15 min	5 min
Number of reference values[3]	min. 12	min. 12	10	12	16	8

5.3 Sensitivity and uncertainty of the model

For Publication III, various modelling choices were tested in modelling of a PVC cable sheath material. The versions tested included the following:

- Reaction scheme (parallel or consecutive)
- Char formation (which reaction produces char)
- Values of the kinetic parameters (A,E) pairs)
- The value of the reaction order
- The fuel yield of the first reaction.

The reaction scheme can typically be either parallel (components degrade independently of each other) or consecutive (one component degrades to another). In some cases, also competing reactions may be relevant. For example, for cellulose degradation, different reaction paths are known to dominate, depending on the temperature and heating rate. At low temperatures, the dominant process is intermolecular dehydration leading to char and gas, and in the presence of air to smouldering combustion. At high temperatures, depolymerisation p
air [119
combina

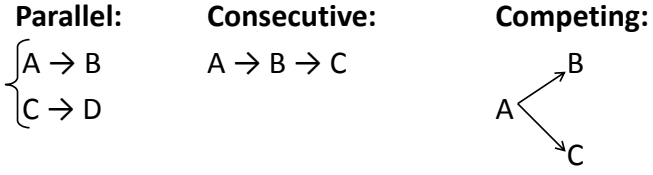

Figure 5.1. Possible reaction paths in pyrolysis modelling.

The reaction path significantly affects the kinetic parameters values, which supports the interpretation that the parameters are model-dependent rather than material properties. Equally good fits can be achieved with any reaction path, but the parameters and the reaction paths cannot be used separately. This difference is clearer with the cone calorimeter results. The consecutive reaction path results in significantly slower degradation when the same thermal parameters are used. This happens because the next reaction is always limited by the previous one in the consecutive reaction path, and at high heating rates and with fixed thermal parameters the reactions overlap more in the parallel path than is possible with the consecutive path. With fitting of the thermal parameters for each reaction path, equally good fit is again reached.

Another modeller decision is that on distribution of char forming. When a parallel reaction path is used, the char can be formed from any reaction(s). On small scale, this does not make any difference, and with the version of FDS (version 5) used for the simulations reported upon in Publication III it did not make any difference on cone calorimeter scale either when the char conductivity was high enough. Version 6 of FDS includes a new ability for modelling swelling surfaces. Char is known to swell and form an insulating layer at the material's surface. The amount of swelling depends on the density of the residue component, and, therefore, it does make a difference at which reaction char is former,

and in what quantities (as seen earlier, in Figure 3.1).

As mentioned above, the values of A and E are unambiguous because of the compensation effect [60], so several pairs that fit equally well can be found. Two sets of parameters (N being 1) were estimated by means of GA and an analytical approach. The results showed that if the reaction path and order are the same, and the kinetic parameters fit equally well on small scale, they cause no difference on the larger scale either. Naturally, small differences in the fit at small scale may lead to larger differences on the larger scale. In addition, this study confirmed that the results are not sensitive to the estimation method, as discussed in Section 5.2, above.

The reaction order is the parameter that compensates for the inaccuracy in modelling of the chemical reactions. In other words, it is the parameter that lumps several reactions together and defines the sharpness of the TGA curve. The results show that this is an important parameter: two sets of parameters that on small scale had equally good fit, resulted in very different heat release and mass loss rate curves in the cone calorimeter context with the same thermal parameters. The lower reaction rate led to slower degradation of the sample material.

Although pure PVC releases only a small quantity of combustible gases during the first reaction, this is often not the case for the real PVC cable material. These materials contain large amounts of additives, including plasticisers that degrade at around the same temperatures as pure PVC (dehydrochlorination reaction), releasing highly flammable gases. This should be taken into account when one builds a PVC model, even if it is not detectable in the TGA results. Alternative methods for defining the fuel yield are presented in Section 4.5, but a fast way to estimate the fuel content of the sample is fitting to the heat release rate curve of the cone calorimeter results. Also making a big difference for the results is whether one allows fuel gas release from the first reaction too.

Summarising the results, one can state that most of the modeller choices do not have any significant effect on the bench scale experimental results but they do have an effect on the parameter values used. This means that the parameters really are model-dependent and should not be considered independent material characteristics, and it means in consequence that these values should not be mixed or used outside the intended application.

5.4 Estimation of the cable composition via MCC

The MCC methods were applied to a PVC sheath of an electric cable (#701) for Publication IV. Now method 2 has been used for estimating the reaction path for another cable, identified as MCMK, which was also used in the sensi-

tivity study of Publication III. The TGA experiments were performed at heating rates of 2, 10, and 20 K/min, and the MCC analysis was repeated three times with a pyrolysis temperature of 75 to 900°C, 900°C combustion temperature, and 20 cm^3/min flow of oxygen to the combustor. In TGA, three clear peaks can be observed and in MCC two. An additional, very weak peak may be observed near the end of the MCC experiment at around 700°C, but it is so weak that it can be ignored. The averages of the experimental results are listed in Table 5.2.

Table 5.2. Experimental MCC results for the MCMK sheath (the values are averages over three repetitions and heating rates).

	Reaction 1	Reaction 2	Reaction 3	Total
T_p $(°C)$	282	462	728	-
$\Delta\alpha$ in TGA	0.56	0.10	0.07	0.74
$\Delta\alpha$ in MCC	-	-	-	0.74
Q/m_0 (MJ/kg) in MCC	10.5	4.2	0	14.7

The iterative estimation process explained in Section 4.5 was repeated $5,000$ times, and the accuracy (or fit) of the final result is $1.5 \cdot 10^{-7}$. The results are listed in Table 5.3, where they are compared with the estimation results for cable #701. The mass fractions in the original material are denoted by Y_i, and the fuel and inert gas yields with $y_{F,ij}$ and $y_{I,ij}$, respectively. Index i is the component index and j the reaction index. The results are quite different: They showed that according to assumptions on the reaction paths, the MCMK to consist of 29% PVC ($i = 1$), 39% plasticiser ($i = 2$) and 32% $CaCO_3$ ($i = 3$), while the corresponding mass fractions for cable #701 are 51% , 27% and 22%, respectively. The experimental results for both cable sheaths are shown in Figure 5.2. From the figures it can be observed that MCMK sheath has less mass loss and higher heat release during the first reaction. This explains the result of the higher mass fraction of plasticiser. The second-reaction mass loss is higher for the #701 sheath, but the heat released during the reactions is almost the same. Hence, the heat of combustion of the PVC residual must be higher. The third mass loss is higher for the MCMK; therefore, the amount of $CaCO_3$ is probably higher in the MCMK. It should be kept in mind that while method 2 allows more truthful reaction paths, the real accuracy always depends on the assumptions made by modeller. The cable sheath compositions presented here may or may not correspond to the real composition, but the resulting model is able to predict correct mass loss and heat release rate using more complex reaction path, as intended.

Table 5.3. Estimation results for MCMK cable sheath compared with the results for cable #701 sheath.

	Estimation boundaries	Initial values	Result (MCMK)	Result (#701)
Y_1	[0.2,0.7]	0.26	0.29	0.51
Y_2	[0.1,0.5]	0.38	0.39	0.27
Y_3	-	0.35	0.32	0.22
y_{I11}	[0.57,0.61]	0.60	0.58	0.60
y_{F11}	[0,0.07]	0.00	0.00	0.04
y_{F12}	[0.5,0.9]	0.85	0.81	0.75
y_{I33}	[0.05,0.3]	0.21	0.22	0.18
$\Delta H_{c,11}$	[25,50]	49.40	32.54	49.10
$\Delta H_{c,12}$	[25,50]	30.38	42.00	35.80
$\Delta H_{c,21}$	[25,50]	30.62	26.90	30.20

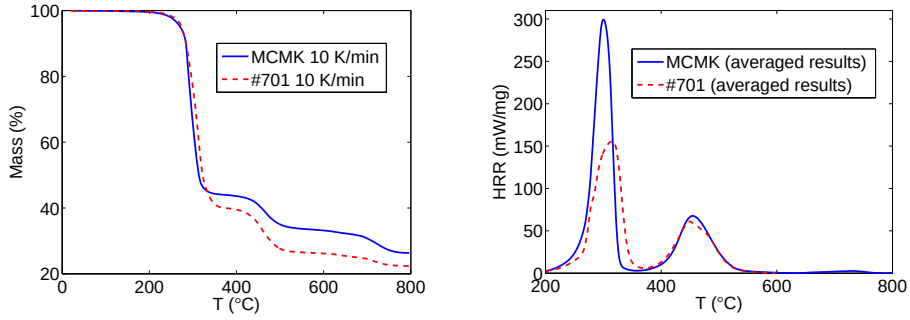

Figure 5.2. Comparison of experimental results for two PVC sheaths. a) TGA at 10 K/min, and b) MCC at 60 K/min.

5.5 Application to a cable tunnel

Publication V applied the parameter estimation results to large scale simulation at a cable tunnel fire of a nuclear power plant. The diversity of the cables found at a real nuclear power plant was taken into account through variation of some of the cable model parameters in the MC simulations. A sensitivity study for the parameter values in cone calorimeter results is presented here.

A cable model used in Publication V was studied via MC technique with the same parameter ranges as in the paper. The sample was generated by means of Latin hypercubes, and the sample size was 100. The variables were the thermal conductivity of the charring pseudocomponents of the sheath (*sheath 1* and *sheath 2*) and the thicknesses of the first three layers (sheath, insulation

plus filler, and sheath). All distributions were assumed to be uniform since the idea was only to study the correlations between input and output. Four output quantities were defined: time to ignition (defined as the time until HRR $> 10\,\mathrm{kW/m^2}$ the first time), maximum heat release rate, time of maximum heat release rate, and time of flame out (the time until HRR $< 10\,\mathrm{kW/m^2}$ in the end of the experiment). The correlations are shown as a scatter plot in Figure 5.3 and as correlation coefficients in Figure 5.4. It can be seen that the thermal conductivity has the greatest correlation with all of the output quantities, and the strongest correlation is with the time of ignition, as expected. The layer thicknesses correlated most strongly with the maximum heat release rate, and the second layer's thickness correlates also with the time of the maximum heat release rate. There is a little uncertainty related to definition of the maximum heat release rate, because of noise in the simulated data. For the flame-out time, the only significant parameter was thermal conductivity.

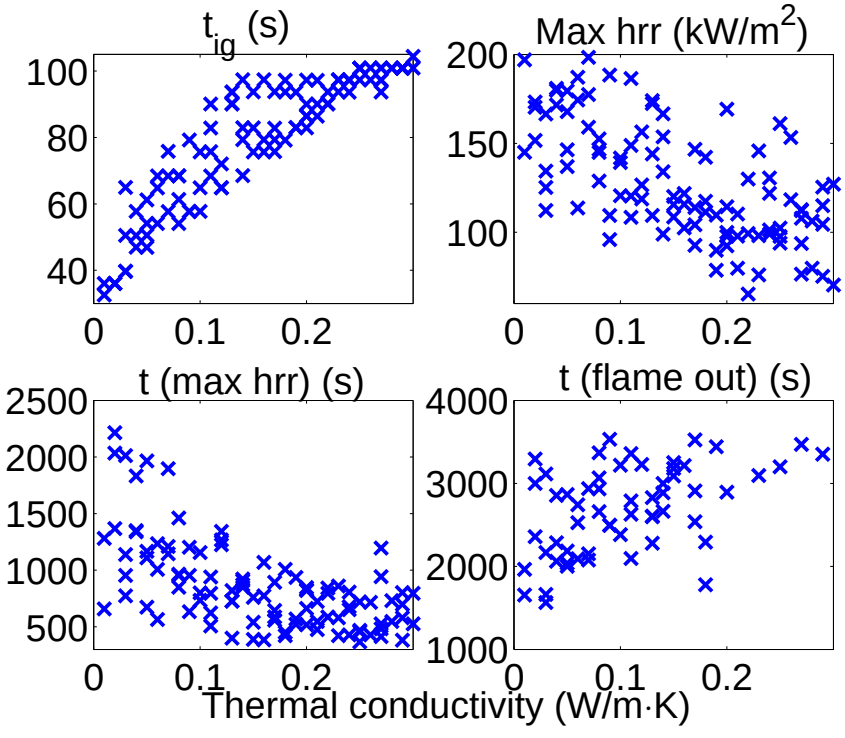

Figure 5.3. Output quantities versus thermal conductivity.

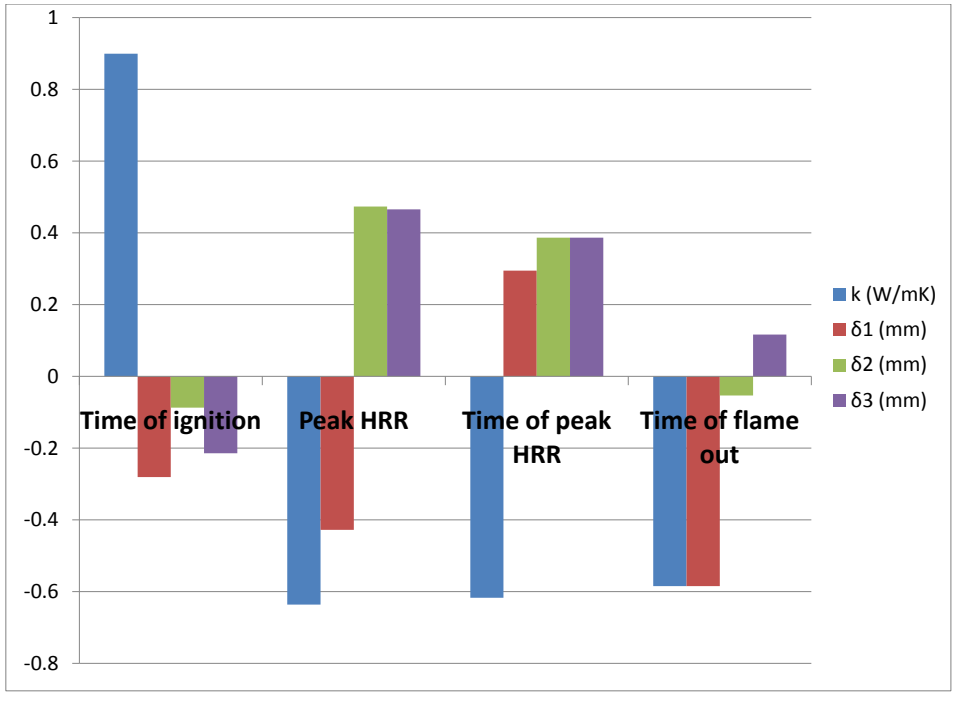

Figure 5.4. Coefficients of correlation between input values and results. k is the thermal conductivity of the first sheath layer, and δ_1, δ_2, and δ_3 are the thicknesses of the three first layers.

6. Conclusions and future work

6.1 Conclusions and discussion

Since fires cause significant harm to people and property, being able to recognise the risks is essential if one is to limit the consequences. For prediction of the fire spread, it is necessary to model the pyrolysis of the solid phase, starting with the chemical degradation reactions. This dissertation has focused on studying the methods of pyrolysis modelling, including the estimation methods, and best practises throughout the modelling process. The methods have been applied to one real-world-scale application in simulation of a cable tunnel fire at a nuclear power plant.

Publication I and Publication II present methods for estimation of the pyrolysis model parameters. The semi-analytical models are simple and fast to use, and they are able to find estimates for the kinetic parameters that show accurate enough fit to the experimental data. Some of them even work for slightly overlapping or noisy data. An additional benefit with these methods is that the result does not depend on the estimation process or on boundary values; the result is always the same. However, for more complicated reaction paths or noisy data, the estimation algorithms offer a more robust method. Those algorithms demand more time and resources but are almost certainly able to find an accurate fit for the experimental data. They can also be used for the estimation of other parameters besides kinetics. The main drawback and criticism of the pyrolysis modelling is that the kinetic parameters are rendered ambiguous by the compensation effect. Depending on the stochastic nature of the algorithm and estimation boundaries, the algorithm may end up reaching a different solution every time. However, the work done in this dissertation project and the discussion above indicate that the bench and large scale results are not sensitive to the kinetic parameters themselves, just relevant for the fit to the experimental data.

Publication III covers the modelling of a PVC material. Several modelling choices are studied there and compared on bench scale. It turned out that the model is sensitive to many choices (e.g., reaction path or order) when the same thermal parameters are used. However, results with equally good fit may be found for all the alternatives if the thermal parameters are fitted separately. This confirms that the parameters are model-specific and not material-specific. It is important that one does not take the parameters out of context and use them in a different model, since they do not mean anything on their own. This

study proved again that any particular estimation method is not significant for finding the fit on the larger scale. As long as the reaction path and order are the same and the result shows equally good fit on the small scale, the difference in order of magnitude does not matter with the pair (A, E).

The methods combining the results of TGA and MCC were presented in Publication IV. These two methods were developed for different modelling needs: method 1 is very simple and can be used only for calculating the correct amount of heat from each reaction. The second method is more complex, and has the ambitious goal of modelling the reaction path as accurately as is reasonable. It can also be used for estimating the composition of an unknown material.

The methods presented in the dissertation were tested in a real world scenario for a nuclear power plant (see Publication V). The cable trays were modelled by means of the genetic algorithm and small and bench scale data. The model was used as a basis for Monte Carlo simulations. The results provided valuable information about the failure probabilities of the cables and the most significant variables behind the most severe conditions. More specifically, this study was used as a part of PRA for an actual nuclear power plant in Finland [4].

The methods and applications developed in this dissertation project have a real impact on the fire safety of the materials and public buildings in use. Capability of accurately modelling and predicting the flame spread with different fire loads improves the evaluation and identification of the risks and makes the allocation of resources more effective. The cable simulations have already contributed to the calculation of more realistic probabilities of fire spread, in the updating of the PRA for the Finnish nuclear power plant. [120]

6.2 Future work and trends in pyrolysis modelling

Work to validate the current fire spread models continues on the large scale. The SGS modelling is expected to solve the current problems found in the CFD modelling of the cables. Being able to model composite structures accurately could save significant amount of effort and expenses in real scale testing in the development phase.

The OECD project PRISME 2[1] will provide excellent large scale experimental results for fires affecting multiple cable trays and electrical cabinets. The tests are performed for various room configurations, and several measurements are made in the course of any given test. The resulting data will be used for validating the entire process of pyrolysis modelling and parameter estimation as described in Section 4.2, from the solid phase thermal degradation reactions

[1] see http://www.oecd-nea.org/jointproj/prisme-2.html

through prediction of fire spread in large installations.

Being able to model the thermal degradation reactions of a material accurately opens new opportunities also in the area of material development and design. Modelling the flame retardancy mechanisms may be especially valuable for the design of new, flame retardant materials. Correctly predicting the cooling effect of an endothermic reaction or the insulating effect of an insulating char barrier enables large scale testing via simulations before the material is even produced. The concentrations of the additives can be studied numerically first, which should decrease the effort of experimental trial and error.

Applications of the presented methods can also be found outside the fire safety engineering. For example, they could be used in developing new methods for extracting biofuels from the biomass as well. Understanding the thermal degradation process of the biomass provides new possibilities for testing the alternative methods by modelling instead of performing experiments. [121–123]

An even smaller scale tool for studying the thermal degradation of materials is molecular dynamics [13]. It calculates the behaviour of the molecules numerically, on the basis of knowledge of the interactions (forces) between the molecules. It allows study on such time and dimension scales as could not be addressed otherwise. The tools of MD could indeed be used in studies of flame retardants. Studying additives' effect in the resin at molecular level may significantly aid in understanding the operation of the current flame retardants and in developing new and better ones.

Bibliography

[1] E. Kokki. Palokuolemat ja ihmisen pelastamiset tulipaloissa 2007–2010. *Pelastusopisto, tutkimusraportti*, 3, 2011.

[2] I. Lopez de Santiago, I. Saez de Ocariz Granja, A. Arbildi Fernandez, F. Fernandez Sanchez, A. Cortes Rueda, and K. Fernandez Horcajo. Fire penetration in an aircraft made in composite. *Proceedings of the Interenational Congress on Combustion and Fire Dynamics in Santander*, 2010.

[3] T. Hakkarainen, J. Hietaniemi, S. Hostikka, T. Karhula, T. Kling, J. Mangs, E. Mikkola, and T. Oksanen. Survivability for ships in case of fire. final report of surship-fire project. *VTT Research Notes 2497*, 2009.

[4] E.-K. Puska and V. Suolanen. Safir 2010. the finnish research programme on nuclear power plant safety 2007-2010. *VTT Research Notes 2571*, 2011.

[5] S.V. Hoa. *Principles of the Manufactoring of Composite Materials*. DEStech Publications, Inc., 2009.

[6] E.S. Papazoglou. Chapter 4. flame retardants for plastics. In C.A. Harper, editor, *Handbook of Building Materials for Fire Protection*, pages 4.1–4.88. McGraw-Hill, New York, 2004.

[7] P. Hornsby. Chapter 7. fire retardant fillers. In C.A. Wilkie and A.B. Morgan, editors, *Fire Retardancy of Polymeric Materials, Second Edition*, page 163–185. CRC PressINC, 2009.

[8] Y. Zhang, Y.C. Wang, C.G. Bailey, and A.P. Taylor. Global modelling of fire protection performance of intumescent coating under different cone calorimeter heating conditions. *Fire Safety Journal*, 50(0):51–62, 2012.

[9] A. Paajanen, T. Korhonen, M. Sippola, S. Hostikka, M. Malendowski, and R. Gutkin. Fds2fem - a tool for coupling fire and structural analyses. *Proceedings of CMM-2013 - Computer Methods in Mechanics, Poznan, Poland*, 2013.

[10] J. Vaari, S. Hostikka, T. Sikanen, and A. Paajanen. Numerical simulations on the performance of waterbased fire suppression systems. *VTT TECHNOLOGY 54*, 2012.

[11] T. Korhonen, S. Hostikka, S. Heliövaara, and H. Ehtamo. Fds+evac: An agent based fire evacuation model. In W.W.F. Klingsch, C. Rogsch, A. Schadschneider, and M. Schreckenberg, editors, *Pedestrian and Evacuation Dynamics 2008*, pages 109–120. Springer Berlin Heidelberg, 2010.

[12] S. Hostikka, T. Kling, and A. Paajanen. Simulation of fire behaviour and human operations using a new stochastic operation time model. *PSAM-11 -ESREL 2012 Conference. 25-29 June. Helsinki*, 2012.

[13] K.D. Smith, M. Bruns, S.I. Stoliarov, M.R. Nyden, O.A. Ezekoye, and P.R. Westmoreland. Assessing the effect of molecular weight on the kinetics of backbone scission reactions in polyethylene using reactive molecular dynamics. *Polymer*, 52(14):3104–3111, 2011.

[14] D. Drysdale. *An Introduction to Fire Dynamics. 3rd edition.* John Wiley and Sons, Ltd, UK., 2011.

[15] C.L. Beyler and M.M. Hirschler. Section 1. chapter 7. thermal decomposition of polymers. In *The SFPE Handbook of Fire Protection Engineering, 2nd edition*, pages 1.99–1.119. National Fire Protection Association, USA, 1995.

[16] Reaction-to-fire tests - heat release, smoke production and mass loss rate. *ISO 5660-1*, 2002.

[17] C. Lautenberger, G. Rein, and C. Fernandez-Pello. The application of a genetic algorithm to estimate material properties for fire modeling from bench-scale fire test data. *Fire Safety Journal*, 41(3):204–214, 2006.

[18] K. McGrattan, S. Hostikka, J. Floyd, H. Baum, R. Rehm, W. Mell, and R. McDermott. *Fire Dynamics Simulator (Version 5) Technical Reference Guide. Volume 1: Mathematical Model*. NIST Special Publication 1018-5.

[19] C. Lautenberger. *A Generalized Pyrolysis Model for Combustible Solids*. PhD thesis, University of California, Berkeley, 2007.

[20] S.I. Stoliarov, S. Crowley, R.E. Lyon, and G.T. Linteris. Prediction of the burning rates of non-charring polymers. *Combustion and Flame*, 156(5):1068–1083, 2009.

[21] L.J. Rodriguez-Aragón and J. López-Fidalgo. Optimal designs for the arrhenius equation. *Chemometrics and Intelligent Laboratory Systems*, 77(1-2):131–138, 2005.

[22] F. Jensen. Activation energies and the arrhenius equation. *Quality and Reliability Engineering International*, 1(1):13–17, 1985.

[23] R.R. Keuleers, J.F. Janssens, and H.O. Desseyn. Comparison of some methods for activation energy determination of thermal decomposition reactions by thermogravimetry. *Thermochimica Acta*, 385(1-2):127–142, 2002.

[24] S. Li and P. Järvelä. Application of a model-free isoconversional method to the cure of phenolic systems. *Journal of Polymer Science Part B: Polymer Physics*, 39(13):1525–1528, 2001.

[25] Z. Liu, Q. Wang, Z. Zou, and G. Tan. Arrhenius parameters determination in non-isothermal conditions for the uncatalyzed gasification of carbon by carbon dioxide. *Thermochimica Acta*, 512(1-2):1–4, 2011.

[26] C. Sierra. Temperature sensitivity of organic matter decomposition in the arrhenius equation: some theoretical considerations. *Biogeochemistry*, 108:1–15, 2012. 10.1007/s10533-011-9596-9.

[27] R. Skomski, R.D. Kirby, and D.J. Sellmyer. Activation entropy, activation energy, and magnetic viscosity. *Journal of Applied Physics*, 85(8):5069–5071, 1999.

[28] D. Stawski and R. Jantas. Potato starch thermooxidation: Selection of the optimal calculation method for activation energy determination. *Potato Research*, 52:355–365, 2009. 10.1007/s11540-009-9139-0.

[29] K.B. McGrattan, T. Kashiwagi, H.R. Baum, and S.L. Olson. Effects of ignition and wind on the transition to flame spread in a microgravity environment. *Combustion and Flame*, 106(4):377–391, 1996.

[30] G. Rein, A. Bar-Ilan, C. Fernandez-Pello, J.L. Ellzey, J.L. Torero, and D.L. Urban. Modeling of one-dimensional smoldering of polyurethane in microgravity conditions. *Proceedings of the Combustion Institute*, 30((2)):2327–2334, 2005. 30th International Symposium of Combustion Institute 2005.

[31] G. Rein, C. Lautenberger, A.C. Fernandez-Pello, J.L. Torero, and D.L. Urban. Application of genetic algorithms and thermogravimetry to determine the kinetics of polyurethane foam in smoldering combustion. *Combustion and Flame*, 146(1-2):95–108, 2006.

[32] S.I. Stoliarov and R.E. Lyon. Thermo-kinetic model of burning. Technical Report DOT/FAA/AR-TN08/17, Federal Aviation Administration, 2008.

[33] R.E. Lyon and R.N. Walters. Pyrolysis combustion flow calorimetry. *Journal of Analytical and Applied Pyrolysis*, 71(1):27–46, 2004.

[34] R.E. Lyon, N.R. Walters, S.I. Stoliarov, and N. Safronava. Principles and practise of microscale combustion calorimetry. Technical Report DOT/FAA/TC-12/53, Federal Aviation Administration, 2013.

[35] S.I. Stoliarov, S. Crowley, R.N. Walters, and R.E. Lyon. Prediction of the burning rates of charring polymers. *Combustion and Flame*, 157(11):2024–2034, 2010.

[36] M. Janssens. Section 3. chapter 2. calorimetry. In *The SFPE Handbook of Fire Protection Engineering, 2nd edition*, pages 3.16–3.36. National Fire Protection Association, USA, 1995.

[37] E. Mikkola. Effects of oxygen concentration on cone calorimeter results. *Proceedings of the Sixth International Interflam Conference*, pages 49–56, 1003.

[38] F. Bell and R. Sizmann. Determination of activation energy from step annealing. *Physica status solidi (b)*, 15(1):369–376, 1966.

[39] J.H. Flynn and L.A. Wall. A quick, direct method for the determination of activation energy from thermogravimetric data. *Journal of Polymer Science Part B: Polymer Letters*, 4(5):323–328, 1966.

[40] H.L. Friedman. New methods for evaluating kinetic parameters from thermal analysis data. *Journal of Polymer Science Part B: Polymer Letters*, 7(1):41–46, 1969.

[41] R.E. Lyon. Heat release kinetics. *Fire and Materials*, 24(4):179–186, 2000.

[42] R.E. Lyon, N. Safronava, and E. Oztekin. A simple method for determining kinetic parameters for materials in fire models. *Fire Safety Science*, 10:765–777, 2011.

[43] K. McGrattan, R. McDermott, W. Mell, G. Forney, J. Floyd, S. Hostikka, and A. Matala. *Proceedings of the 12^{th} International Interflam Conference*.

[44] R. Sundberg. Statistical aspects on fitting the arrhenius equation. *Chemometrics and Intelligent Laboratory Systems*, 41(2):249–252, 1998.

[45] J.V. Li, S.W. Johnston, Y. Yan, and D.H. Levi. Measuring temperature-dependent activation energy in thermally activated processes: A 2d arrhenius plot method. *Review of Scientific Instruments*, 81(3):033910, 2010.

[46] O. E. Rodionova and A. L. Pomerantsev. Estimating the parameters of the arrhenius equation. *Kinetics and Catalysis*, 46:305–308, 2005. 10.1007/s10975-005-0077-9.

[47] M. Starink. Activation energy determination for linear heating experiments: deviations due to neglecting the low temperature end of the temperature integral. *Journal of Materials Science*, 42:483–489, 2007. 10.1007/s10853-006-1067-7.

[48] Z. Gao, T. Kaneko, D. Hou, and M. Nakada. Kinetics of thermal degradation of poly(methyl methacrylate) studied with the assistance of the fractional conversion at the maximum reaction rate. *Polymer Degradation and Stability*, 84(3):399–403, 2004.

[49] M. Chaos, M.M. Khan, N. Krishnamoorthy, J.L. de Ris, and S.B. Dorofeev. Evaluation of optimization schemes and determination of solid fuel properties for cfd fire models using bench-scale pyrolysis tests. *Proceedings of the Combustion Institute*, 33:2599–2606, 2011.

[50] C. Lautenberger and C. Fernandez-Pello. Optimization Algorithms for Material Pyrolysis Property Estimation. *Fire Safety Science*, 10:751–764, 2011.

[51] T. Mani, P. Murugan, and N. Mahinpey. Determination of distributed activation energy model kinetic parameters using simulated annealing optimization method for nonisothermal pyrolysis of lignin. *Industrial and Engineering Chemistry Research*, 48(3):1464–1467, 2009.

[52] B. Saha, P.K. Reddy, and A.K. Ghoshal. Hybrid genetic algorithm to find the best model and the globally optimized overall kinetics parameters for thermal decomposition of plastics. *Chemical Engineering Journal*, 138(1–3):20–29, 2008.

[53] R.D. Webster. Pyrolysis model parameter optimization using a customized stochastic hill-climber algorithm and bench scale fire test data. Master's thesis, Graduate school of the University of Maryland, Collegepark, 2009.

[54] Q.Y. Duan, V.K. Gupta, and S. Sorooshian. Shuffled complex evolution approach for effective and efficient global minimization. *Journal of Optimization Theory and Applications*, 76:501–521, 1993.

[55] T.A. El-Mihoub, A.A. Hopgood, L. Nolle, and A. Battersby. Hybrid genetic algorithms: A review. *Engineering Letters*, 13(2):124–137, 2006.

[56] C.-H. Wang and J.-Z. Lu. A hybrid genetic algorithm that optimizes capacitated vehicle routing problems. *Expert Systems with Applications*, 36(2, Part 2):2921–2936, 2009.

[57] G. Whittaker, R. Confesor Jr., S.M. Griffith, R. Färe, S. Grosskopf, J.J. Steiner, G.W. Mueller-Warrant, and G.M. Banowetz. A hybrid genetic algorithm for multiobjective problems with activity analysis-based local search. *European Journal of Operational Research*, 193(1):195–203, 2009.

[58] F. Jin, S. Song, and C. Wu. A simulated annealing algorithm for single machine scheduling problems with family setups. *Computers and Operations Research*, 36(7):2133–2138, 2009.

[59] R. Tavakkoli-Moghaddam, A.R. Rahimi-Vahed, A. Ghodratnama, and A. Siadat. A simulated annealing method for solving a new mathematical model of a multi-criteria cell formation problem with capital constraints. *Advances in Engineering Software*, 40(4):268–273, 2009.

[60] A.V. Nikolaev, V.A. Logvinekol, and V.M. Gorbatchevl. Special features of the compensation effect in non-isothermal kinetics of solid-phase reactions. *Journal of Thermal Analysis and Calorimetry*, 6(4):473–477, 1974.

[61] A.K. Galwey and M.E. Brown. Arrhenius parameters and compensation behaviour in solid-state decompositions. *Thermochimica Acta*, 300(1-2):107–115, 1997.

[62] R.E. Lyon and N. Safronava. A comparison of direct methods to determine n-th order kinetic parameters of solid thermal decomposition for use in fire models. *Journal of Thermal Analysis and Calorimetry*, 114(1):213–227, 2013.

[63] J.R. Opfermann, E. Kaisersberger, and H.J. Flammersheim. Model-free analysis of thermoanalytical data-advantages and limitations. *Thermochimica Acta*, 391(1–2):119 – 127, 2002.

[64] D.P. Landau and K. Binder. *A Guide To Monte Carlo Simulations In Statistical Physics*. Cambridge University Press, 2000.

[65] N. Metropolis and S. Ulam. *Journal of the American Statistical Association*. Number vol. 44. American Statistical Association, 1949.

[66] M.D. McKay, R.J. Beckman, and W.J. Conover. A comparison of three methods for selecting values of input variables in the analysis of output from a computer code. *Technometrics*, 1979.

[67] M. Stein. Large sample properties of simulations using latin hypercube sampling. *Technometrics*, 29(2):143–151, 1987.

[68] S. Hostikka and O. Keski-Rahkonen. Probabilistic simulation of fire scenarios. *Nuclear Engineering and Design*, 224(3):301–311, 2003.

[69] S. Hostikka, T. Korhonen, and O. Keski-Rahkonen. Two-model monte carlo simulation of fire scenarios. *Fire Safety Science*, 8:1241–1252, 2005.

[70] R.E. Lyon. Chapter 3. plastics and rubber. In C.A. Harper, editor, *Handbook of Building Materials for Fire Protection*, pages 3.1–3.51. McGraw-Hill, New York, 2004.

[71] K. McGrattan et al. *Fire Dynamics Simulator User's Guide.* NIST Special Publication 1019.

[72] D. Price, G. Anthony, and P. Carty. Chapter 1. introduction: polymer combustion, condensed phase pyrolysis and smoke formation. In A.R. Horrocs and D. Price, editors, *Fire retardant materials*, pages 10–30. Woodhead Publishing Limited, England, 2001.

[73] M. Lewin and E.D. Weil. Chapter 2. mechanism and models of action in flame retardancy of polymers. In A.R. Horrocs and D. Price, editors, *Fire retardant materials*, pages 31–68. Woodhead Publishing Limited, England, 2001.

[74] S.V. Levchik. Chapter 1. introduction to flame retardancy and polymer flammability. In A.B. Morgan and C.A. Wilkie, editors, *Flame Retardant Polymer Nanocomposites*, pages 1–30. Wiley, 2007.

[75] P. Georlette. Chapter 8. applications of halogen flame retardants. In A.R. Horrocs and D. Price, editors, *Fire retardant materials*, pages 264–292. Woodhead Publishing Limited, England, 2001.

[76] R.P. Lattimer and W.J. Kroenke. The formation of volatile pyrolyzates form poly(vinyl chloride). *Journal of Applied Polymer Science*, 25(1):101–110, 1980.

[77] G. Montaudo and C. Puglisi. Evolution of aromatics in the thermal degradation of poly(vinyl chloride): A mechanistic study. *Polymer Degradation and Stability*, 33(2):229–262, 1991.

[78] A. Marcilla and M. Beltran. Pvc-plasticizer interactions during the thermal decomposition of pvc plastisols. influence of the type of plastizicer and resin. *Polymer Degradation and Stability*, 53(2):261–268, 1996.

[79] A. Jimenez, J. Lopez, J. Vilaplana, and H.-J. Dussel. Thermal degradation of plastisols. effect of some additives on the evolution of gaseous products. *Journal of Analytical and Applied Pyrolysis*, 40–41(0):201–215, 1997.

[80] E.O. Elakesh, T.R. Hull, D. Price, G.J. Milnes, and P. Carty. Effect of plasticizers on the thermal decomposition of chlorinated polyvinylchloride. *Journal of Vinyl and Additive Technology*, 11(1):21–27, 2005.

[81] A. Marcilla and M. Beltran. Effect of the plasticizer concentration and heating rate on the thermal decomposition behaviour of pvc plastisols. kinetic analysis. *Polymer Degradation and Stability*, 60(1):1–10, 1998.

[82] R. Miranda, J. Yang, C. Roy, and C. Vasile. Vacuum pyrolysis of pvc i. kinetic study. *Polymer Degradation and Stability*, 64(1):127–144, 1999.

[83] M. Benes, V. Plaek, G. Matuschek, A. A. Kettrup, K. Gyoryova, W. D. Emmerich, and V. Balek. Lifetime simulation and thermal characterization of pvc cable insulation materials. *Journal of Thermal Analysis and Calorimetry*, 82(3):761–768, 2005.

[84] A. Marcilla and M. Beltran. Thermogravimetric kinetic study of poly-(vinyl chloride) pyrolysis. *Polymer Degradation and Stability*, 48(2):219–229, 1995.

[85] A. Marcilla and M. Beltran. Kinetic models for the thermal decomposition of commercial pvc resins and plasticizers studied by thermogravimetric analysis. *Polymer Degradation and Stability*, 53(2):251–260, 1996.

[86] M. Beltran and A. Marcilla. Kinetic models for the thermal decomposition of pvc plastisols. *Polymer Degradation and Stability*, 55(1):73 – 87, 1997.

[87] S. Kim. Pyrolysis kinetics of waste pvc pipe. *Waste Management*, 21(7):609–616, 2001.

[88] G. Wypych. *PVC Formulary*. ChemTec Publishing, 2009.

[89] N.N. Greenwood and A. Earnshaw. *Chemistry of the Elements*. Pergamon Press Ltd, 1984.

[90] M. Pansu and J. Gautheyrou. Chapter 17. carbonates. In *Handbook of Soil Analysis*, pages 593–604. Springer Berlin Heidelberg, 2006.

[91] K. McGrattan, A. Lock, N. Marsh, M. Nyden, Bareham S., M. Price, A.B. Morgan, M. Galaska, K. Schenck, and D. Stroup. Cable heat release, ignition, and spread in tray installations during fire (christifire), phase 1: Horizontal trays. *NUREG/CR-7010*, 1, 2012.

[92] N. Alvares and C. Fernandez-Pello. Fire initiation and spread in overloaded communication system cable trays. *Experimental Thermal and Fluid Science*, 21(1-3):51–57, 2000.

[93] P. Van Hees, J. Axelsson, A. M. Green, and S. J. Grayson. Mathematical modelling of fire development in cable installations. *Fire and Materials*, 25(4):169–178, 2001.

[94] P. Andersson and P. Van Hees. Performance of cables subjected to elevated temperatures. *Fire Safety Science*, 8:1121–1132, 2005.

[95] K. McGrattan and J. Dreisbach. Cable response to live fire (carolfire) volume 3: Thermally-induced electrical failure (thief) model. *NUREG/CR-6931*, 3, 2008.

[96] S.P. Nowlen. The impact of thermal aging on the flammability of electric cables. *NUREG/CR-5629, SAND90-2121*, 1991.

[97] J. Mangs and A. Matala. Ageing effects on flame spread and pyrolysis of pvc cables. *VTT Research Reports VTT-T-07229-10*, 2010.

[98] V. Placek and T. Kohout. Comparison of cable ageing. *Radiation Physics and Chemistry*, 79(3):371–374, 2010. IONIZING RADIATION AND POLYMERS Proceedings of the 8th International Symposium on Ionizing Radiation and Polymers Angra dos Reis, Rio de Janeiro, Brazil, 12-17 October 2008.

[99] D.D.L. Chung. *Composite Materials. Science and Applications. 2nd edition.* Springer, USA., 2010.

[100] A.P. Mouritz and A.G. Gibson. *Fire Properties of Polymer Composite Materials*. Springer, The Netherlands, 2006.

[101] Karbhari V.M. and Seible F. Fiber reinforced composites - advanced materials for the renewal of civil infrastructure. *Applied Composite Materials*, 7(2/3):95–124, 2000.

[102] K.G. Satyanarayana, G.G.C. Arizaga, and F. Wypych. Biodegradable composites based on lignocellulosic fibers—an overview. *Progress in Polymer Science*, 34(9):982–1021, 2009.

[103] T. Ford. Aerospace composites. *Aircraft Engineering and Aerospace Technology*, 69(4):334–342, 1997.

[104] G. Savage. Formula 1 composites engineering. *Engineering Failure Analysis*, 17(1):92–115, 2010.

[105] S. Bocchini and G. Camino. Chapter 4. halogen-containing flame retardants. In C.A. Wilkie and A.B. Morgan, editors, *Fire Retardancy of Polymeric Materials, Second Edition*, pages 75–105. CRC PressINC, 2009.

[106] P. Joseph and J.R. Ebdon. Chapter 5. phosphorus-based flame retardants. In C.A. Wilkie and A.B. Morgan, editors, *Fire Retardancy of Polymeric Materials, Second Edition*, pages 107–127. CRC PressINC, 2009.

[107] S. Bourbigot and S. Duquesne. Chapter 6. intumescence-based fire retardants. In C.A. Wilkie and A.B. Morgan, editors, *Fire Retardancy of Polymeric Materials, Second Edition*, pages 129–162. CRC PressINC, 2009.

[108] G.S. Springer. Model for predicting the mechanical properties of composites at elevated temperatures. *Journal of Reinforced Plastics and Composites*, 3(1):85–95, 1984.

[109] Y. Bai and T. Keller. Modeling of mechanical response of frp composites in fire. *Composites Part A: Applied Science and Manufacturing*, 40(6–7):731 – 738, 2009.

[110] N.A. Dembsey and D.J. Jacoby. Evaluation of common ignition models for use with marine cored composites. *Fire and Materials*, 24(2):91–100, 2000.

[111] B. Lattimer and T. Cambell. Chapter 4. fire modelling of composites. In Gibson A.G. Mouritz, A.P., editor, *Fire Properties of Polymer Composite Materials*, pages 103–132. Springer, The Netherlands, 2006.

[112] E. Kim, C. Lautenberger, and N. Dembsey. Property estimation for pyrolysis modeling applied to polyester frp composites with different glass contents. *Composites and Polycon 2009. American Composites Manufacturers Association*, 2009.

[113] C. Lautenberger, E. Kim, N. Dembsey, and C. Fernandez-Pello. The role of decomposition kinetics in pyrolysis modeling - application to a fire retardant polyester composite. *Fire Safety Science*, 9:1201–1212, 2009.

[114] J. Trelles and B.Y. Lattimer. Modelling thermal degradation of composite materials. *Fire and Materials*, 31(2):147–171, 2007.

[115] J. Opfermann. Kinetic analysis using multivariate non-linear regression. i. basic concepts. *Journal of Thermal Analysis and Calorimetry*, 60(2):641–658, 2000.

[116] S.I. Stoliarov, N. Safronava, and R.E. Lyon. The effect of variation in polymer properties on the rate of burning. *Fire and Materials*, 33(6):257–271, 2009.

[117] K. McGrattan et al. *Fire Dynamics Simulator Volume 2: Verification.* NIST Special Publication 1018.

[118] K. McGrattan et al. *Fire Dynamics Simulator Volume 3: Validation.* NIST Special Publication 1018.

[119] C. Di Blasi. Physico-chemical processes occurring inside a degrading two-dimensional anisotropic porous medium. *International Journal of Heat and Mass Transfer*, 41(24):4139–4150, 1998.

[120] L. Tunturivuori. Updating of the fire pra of the olkiluoto npp units 1 and 2. *PSAM-11 -ESREL 2012 Conference. 25-29 June. Helsinki*, 2012.

[121] D. Mohan, C.U. Pittman, and P.H. Steele. Pyrolysis of wood-biomass for bio-oil: A critical review. *Energy & Fuels*, 20(3):848–889, 2006.

[122] C. Di Blasi. Modeling chemical and physical processes of wood and biomass pyrolysis. *Progress in Energy and Combustion Science*, 34(1):47–90, 2008.

[123] C. Di Blasi. Combustion and gasification rates of lignocellulosic chars. *Progress in Energy and Combustion Science*, 35(2):121–140, 2009.

Series title and number
VTT Science 44

Title	**Methods and applications of pyrolysis modelling for polymeric materials**
Author(s)	Anna Matala
Abstract	Fire is a real threat for people and property. However, if the risks can be identified before the accident, the consequences can be remarkably limited. The requirement of fire safety is particularly important in places with large number of people and limited evacuation possibilities (e.g., ships and airplanes) and for places where the consequences of fire may spread wide outside of the fire location (e.g., nuclear power plants). The prerequisite for reliable fire safety assessment is to be able to predict the fire spread instead of prescribing it. For predicting the fire spread accurately, the pyrolysis reaction of the solid phase must be modelled. The pyrolysis is often modelled using the Arrhenius equation with three unknown parameters per each reaction. These parameters are not material, but model specific, and therefore they need to be estimated from the experimental small-scale data for each sample and model individually. The typical fuel materials in applications of fire safety engineers are not always well-defined or characterised. For instance, in electrical cables, the polymer blend may include large quantities of additives that change the fire performance of the polymer completely. Knowing the exact chemical compound is not necessary for an accurate model, but the thermal degradation and the release of combustible gases should be identified correctly. The literature study of this dissertation summarises the most important background information about pyrolysis modelling and the thermal degradation of the polymers needed for understanding the methods and results of this dissertation. The articles cover developing methods for pyrolysis modelling and testing them for various materials. The sensitivity of the model for the modelling choices is also addressed by testing several typical modeller choices. The heat release of unknown polymer blend is studied using Microscale Combustion Calorimetry (MCC), and two methods are developed for effectively using the MCC results in building an accurate reaction path. The process of pyrolysis modelling is presented and discussed. Lastly, the methods of cable modelling are applied to a large scale simulation of a cable tunnel of a Finnish nuclear power plant. The results show that the developed methods are practical, produce accurate fits for the experimental results, and can be used with different materials. Using these methods, the modeller is able to build an accurate reaction path even if the material is partly uncharacterised. The methods have already been applied to simulating real scale fire scenarios, and the validation work is continuing.
ISBN, ISSN	ISBN 978-951-38-8101-6 (Soft back ed.) ISBN 978-951-38-8102-3 (URL: http://www.vtt.fi/publications/index.jsp) ISSN-L 2242-119X ISSN 2242-119X (Print) ISSN 2242-1203 (Online)
Date	November 2013
Language	English, Finnish abstract
Pages	85 p. + app 87 p.
Keywords	pyrolysis modelling, simulation, polymer, cables, composites, probabilistic risk assessment (PRA)
Publisher	VTT Technical Research Centre of Finland P.O. Box 1000, FI-02044 VTT, Finland, Tel. +358 20 722 111

Julkaisun sarja ja numero
VTT Science 44

Nimeke	**Pyrolyysimallinnuksen metodeita ja sovelluksia polymeereille**
Tekijä(t)	Anna Matala
Tiivistelmä	Tulipalot aiheuttavat todellisen uhan ihmisille ja omaisuudelle. Mikäli riskit voidaan tunnistaa jo ennen onnettomuutta, tulipalon ikäviä seurauksia voidaan rajoittaa. Paloturvallisuuden merkitys korostuu erityisesti paikoissa, joissa on paljon ihmisiä ja rajoitetut evakuointimahdollisuudet (esim. laivat ja lentokoneet), ja laitoksissa, joissa tulipalon seuraukset voivat levitä laajalle palopaikan ulkopuolellekin (esim. ydinvoimalaitokset). Jotta materiaalien palokäyttäytymistä voitaisiin luotettavasti tarkastella erilaisissa olosuhteissa, pitää palon leviäminen pystyä ennustamaan sen sijaan, että paloteho määrättäisiin ennalta. Palon leviämisen ennustamiseksi täytyy materiaalin kiinteän faasin pyrolyysireaktiot tuntea ja mallintaa. Pyrolyysi mallinnetaan usein käyttäen Arrheniuksen yhtälöä, jossa on kolme tuntematonta parametria jokaista reaktiota kohti. Nämä parametrit eivät ole materiaali- vaan mallikohtaisia, ja siksi ne täytyy estimoida kokeellisista pienen mittakaavan kokeista jokaiselle näytteelle ja mallille erikseen. Paloturvallisuusinsinöörin kannalta erityisen hankalaa on, että palavat materiaalit eivät useinkaan ole hyvin määriteltyjä tai tunnettuja. Esimerkiksi sähkökaapeleiden polymeeriseokset voivat sisältää suuria määriä erilaisia lisäaineita, jotka vaikuttavat materiaalin palokäyttäytymiseen merkittävästi. Kemiallisen koostumuksen tunteminen ei ole välttämätöntä luotettavan mallin aikaansaamiseksi, mutta aineen lämpöhajoaminen ja erityisesti palavien kaasujen vapautuminen tulisi tuntea tarkasti. Väitöskirjan tiivistelmäosa kokoaa yhteen tärkeimmät taustatiedot pyrolyysimallinnuksen ja polymeerien palokäyttäytymisen ymmärtämisen tueksi. Tässä väitöstyössä on kehitetty menetelmiä pyrolyysiparametrien estimoimiseksi ja näitä metodeita on testattu erilaisilla materiaaleilla. Mallinnusvalintojen merkitystä mallin tarkkuuteen on myös tutkittu herkkyysanalyysin keinoin. Osittain tuntemattomien polymeeriseosten lämmön vapautumista on tutkittu käyttäen mikrokalorimetria. Mikrokalorimetritulosten hyödyntämiseksi kehitettiin kaksi metodia, joiden avulla voidaan saada aikaan entistä tarkempia reaktiopolkuja. Lopuksi pyrolyysimallinnusta on hyödynnetty sovellusesimerkissä suomalaisen ydinvoimalan kaapelitilan täyden mittakaavan kaapelisimuloinneissa. Tulokset osoittavat, että tässä työssä kehitetyt menetelmät ovat käytännöllisiä, tuottavat riittävän tarkkoja sovituksia koetuloksille ja niitä voidaan soveltaa monien erilaisten materiaalien mallintamiseen. Näitä menetelmiä käyttämällä mallintaja pystyy mallintamaan tuntemattomienkin materiaalien palokäyttäytymistä riittävän tarkasti. Menetelmiä on jo sovellettu todellisten, suuren mittakaavan palotilanteiden simuloimiseksi, ja validointityö jatkuu edelleen.
ISBN, ISSN	ISBN 978-951-38-8101-6 (nid.) ISBN 978-951-38-8102-3 (URL: http://www.vtt.fi/publications/index.jsp) ISSN-L 2242-119X ISSN 2242-119X (painettu) ISSN 2242-1203 (verkkojulkaisu)
Julkaisuaika	Marraskuu 2013
Kieli	Englanti, suomenk. tiivistelmä
Sivumäärä	85 s. + liitt. 87 s.
Avainsanat	pyrolyysimallinnus, simulaatiot, polymeerit, kaapelit, komposiitit, todennäköisyyspohjainen riskianalyysi (PRA)
Julkaisija	VTT PL 1000, 02044 VTT, puh. 020 722 111